Universidade de Aveiro Departamento de Química
2017

Daniel Martins Cordeiro

Desenvolvimento de membranas compósitas à base de celulose bacteriana para pilhas de combustível microbianas

Universidade de Aveiro Departamento de Química
2017

Daniel Martins Cordeiro

Desenvolvimento de membranas compósitas à base de celulose bacteriana para pilhas de combustível microbianas

Tese apresentada à Universidade de Aveiro para cumprimento dos requisitos necessários à obtenção do grau de Mestre em Biotecnologia, ramo Industrial e Ambiental, realizada sob a orientação científica da Doutora Carla Andreia Cunha Vilela, Investigadora de Pós-Doutoramento do CICECO – Instituto de Materiais de Aveiro e do Departamento de Química da Universidade de Aveiro e da Doutora Carmen Sofia da Rocha Freire Barros, Investigadora Principal do CICECO – Instituto de Materiais de Aveiro e do Departamento de Química da Universidade de Aveiro.

Dedicar este trabalho à entidade, qualquer que ela seja, que permite que após 400 anos de método científico, e com milhões de cientistas a investigar nos entretantos, ainda existam temas novos nos quais trabalhar. E que assim continue!

E, como não podia deixar de ser, aos meus pais, investidores a fundo perdido por excelência.

o júri

Presidente

Professora Doutora Luísa Alexandra Seuanes Serafim Martins Leal
Professora Auxiliar da Universidade de Aveiro

Doutor Filipe Miguel Henriques Lebre Ramos Figueiredo
Investigador Principal da Universidade de Aveiro

Doutora Carla Andreia Cunha Vilela
Investigadora de Pós-Doutoramento da Universidade de Aveiro

agradecimentos

Agradecer às minhas orientadoras Carla Vilela e Carmen Freire pelo acompanhamento, paciência e estímulo à autonomia.
À Paula Barbosa pela ajuda com as medidas de condutividade protónica.
Ao Ricardo Pinto pela ajuda com a microscopia eletrónica de varrimento.
Ao CICECO – Instituto de Materiais do Departamento de Química e da Universidade de Aveiro pelo apoio material e disponibilização do laboratório.
À professora Alexandra Rodrigues Pinto e à Joana Vila Boas do Departamento de Engenharia Química da FEUP – Faculdade de Engenharia da Universidade do Porto pela parceria e realização dos testes em pilhas de combustível microbianas.

palavras-chave

Celulose bacteriana, ácido poli(estireno sulfónico), compósitos de matriz polimérica, membranas de permuta protónica, pilhas de combustível microbianas.

resumo

As pilhas de combustível microbianas constituem uma tecnologia com a potencialidade de produção de energia elétrica com simultâneo tratamento de efluentes. Esta potencialidade assume particular relevância num mundo que cada vez mais procura soluções ecológicas e sustentáveis para a produção de eletricidade. Neste sentido, o desenvolvimento de membranas de permuta protónica com base em celulose bacteriana (BC) irá contribuir para aumentar o caráter ecológico das pilhas de combustível microbianas (MFCs). O presente trabalho tem por objetivo o desenvolvimento de membranas compósitas baseadas em BC e no ácido poli(4-estireno sulfónico) (PSSA) para aplicação em MFCs. Deste modo, a produção, caraterização e aplicação de membranas de PSSA/BC numa pilha de combustível microbiana é descrita como uma abordagem relevante à produção de eletricidade por microrganismos com recurso a materiais de base biológica. O polímero PSSA foi incorporado com sucesso na estrutura tridimensional da BC através da polimerização radicalar *in situ* do monómero ácido 4-estirenosulfónico na presença de um agente reticulante. Estas membranas compósitas apresentam uma capacidade de troca iónica de 1,85 ± 0,83 $mmol.g^{-1}$ e condutividades protónicas máximas de 17,3 $mS.cm^{-1}$ (94 ºC, 98% humidade relativa, configuração através-do-plano) e 344 $mS.cm^{-1}$ (80 ºC, 98% humidade relativa, configuração em-plano). Estes resultados demonstram um comportamento anisotrópico da condutividade protónica das membranas compósitas dependente da configuração em que é medida. A aplicação de uma membrana de PSSA/BC numa pilha de combustível microbiana originou uma potencia máxima de 2,42 $mW.m^{-2}$, uma voltagem de circuito aberto de 0,436 V e uma resistência interna de $1{,}51\times10^{4}$ Ω. Estes valores são superiores aos obtidos com uma membrana comercial de Nafion®.

keywords

Bacterial cellulose, poly(styrene sulfonic acid), polymer matrix composites, proton exchange membranes, microbial fuel cells.

abstract

Microbial fuel cells are a technology with the potentiality to be used on the production of electricity while simultaneously treating effluents. This potentiality is particularly relevant in a world that actively searches for ecological and sustainable solutions for electricity production. In this sense, the development of proton exchange membranes based on bacterial cellulose (BC) can contribute to increase the ecological character of microbial fuel cells (MFCs). The present work has the objective of developing nanocomposite membranes based on BC and poly(4-styrene sulfonic acid) (PSSA) for application on MFCs. As such, the production, characterization and application of PSSA/BC membranes in a MFC is described as a relevant approach on the production of electricity by microorganisms and with the resort to bio-based materials. The PSSA polymer was successfully incorporated into the BC three-dimensional structure by the *in situ* free radical polymerization of the 4-styrene sulfonic acid monomer in the presence of a cross-linking agent. This nanocomposite membrane shows an ionic exchange capacity of 1.85 ± 0.83 $mmol.g^{-1}$ and maximum protonic conductivities of 17.3 $mS.cm^{-1}$ (94 ºC, 98% relative humidity (RH), through-plane configuration) and 344 $mS.cm^{-1}$ (80 ºC, 98% RH, in-plane configuration). These results show a nanocomposite membrane with anisotropic proton conductance behaviour dependant on the configuration in which the protonic conductivity is measured. The PSSA/BC application on a single-chamber MFC yielded a maximum power density of 2.42 $mW.m^{-2}$, an open circuit voltage of 0.436 V and an internal resistance of 1.51×10^{4} Ω. These results are superior than those obtained with a commercial Nafion® membrane.

Outline

Figures

Tables

Abbreviations

AEM	Anion exchange membrane
AFC	Alkaline fuel cell
ATP	Adenosine triphosphate
BC	Bacterial cellulose
CFU	Colony forming units
COD	Chemical oxygen demand
DET	Direct electron transfer
DFFC	Direct fuelled fuel cell
DMFC	Direct methanol fuel cell
FAD^+	Flavin adenine dinucleotide
FMN^+	Flavin mononucleotide
FTIR-ATR	Fourier transform infrared-attenuated total reflectance
GRAS	Generally recognized as safe
Hap	Hydroxyapatite
HS	Hestrin-Schramm
KPS	Potassium persulfate
IEC	Ionic exchange capacity
IS	Impedance spectroscopy
MCFC	Molten carbonate fuel cell
MEA	Membrane-electrode assembly
MET	Mediated electron transfer
MFC	Microbial fuel cell
MOEP	Methacryloyloxyethyl phosphate
NAD^+	Nicotinamide adenine dinucleotide
NMMO	*N*-methyl-morpholine *N*-oxide
NP	Nanoparticles
OCV	Open-circuit voltage
OLED	Organic light emitting diodes
PAFC	Phosphoric acid fuel cell
PAMPS	Poly(2-acrylamido-2-methyl-1-propanesulphonic acid)
PANI	Polyaniline
PEGDA	Poly(ethylene glycol diacrylate)

PEM	Proton exchange membrane
PEMFC	Proton exchange membrane fuel cell
PFSI	Perfluorosulphonic ionomer
PHEMA	Poly(2-hydroxyethyl methacrylate)
PMOEP	Poly(methacryloyloxyethyl phosphate)
PPy	Polypyrrole
PSSA	Poly(4-styrene sulphonic acid)
PTFE	Poly(tetrafluoroethylene)
PVA	Poly(vinyl alcohol)
RH	Relative humidity
SEM	Scanning electronic microscopy
UV	Ultra violet
VTF	Vogel-Tamman-Fulcher

1. Introduction

1.1. The Context

In a technological society with an ever-increasing demand for energy, the efficiency with which different forms of storing energy are converted between each other is as relevant as the abundance of the primary sources of that same energy. In this context, the fuel cell technology supplies a generally more efficient way to convert energy stored in chemical compounds into a directly consumable energy, electricity, when compared with the widespread traditional technologies.

The availability of large quantities of unharnessed energetic potential in organic compounds further increased the scope of the fuel cell technology with the development of microbial fuel cells. These are devices that take advantage of the biocatalytic abilities of microorganisms to produce electricity from the microorganism-mediated oxidation of organic substrates. Simultaneously, the ecological and sustainable nature of microbial fuel cell operation and electricity production further increased the interest and potential of microbial fuel cells application.

However, one of the microbial fuel cell key components, the proton exchange membrane, is remarkable for its high costs, namely when made of perfluorosulphonic ionomers. As a more ecological alternative for proton exchange membrane production, bacterial cellulose-based composites were developed, with focus on the proton conducting properties of these composite materials. In this sense, two groups of composite materials were used, bacterial celluloses functionalized with phosphoric acid, described in the works of Gaopeng Jiang *et al*., 2012 and Vilela *et al*., 2016, and compounds functionalized with sulphonic groups, developed in the works of Gadim *et al*., 2014, 2015 and 2017 Gaopeng Jiang *et al*., 2015 and Lin *et al*, 2013.

The purpose of this work is to continue the study of the membranes developed by Gadim *et al*., 2014 by applying them as proton exchange membranes in microbial fuel cells. As such, in this work a broad theoretical framework of the fuel cell technology and on the subject of bacterial cellulose is provided, followed by the description of the preparation, characterization and, finally, application of poly(4-styrene sulfonic acid)/bacterial cellulose composite membranes on a microbial fuel cell.

1.2. Conventional fuel cells

Fuel cells are devices that perform the conversion of energy stored in chemical compounds into electric energy. Batteries and combustion engines are two alternative technologies to perform this conversion **(Sharaf & Orhan, 2014)**. Combustion engines produce energy as work through oxidation by means of fuel combustion (*e.g.*, fossil fuels); this energy is afterwards converted into electric energy by an electrical power generator. This multi-step conversion has low efficiencies, which are further limited by the theoretical Carnot efficiency. In addition, combustion engines produce noise, vibrations and pollutant gases, including greenhouse effect gases. In batteries, electric energy is produced typically by the oxidation of metallic electrodes, in a mild acid electrolyte, upon which exhaustion, batteries must be discarded or recharged, considering that the battery focus is on energy storage rather than energy conversion. Moreover, batteries are susceptible to deterioration and variations in energy output in different phases of their life cycle. On the other hand, fuel cells show some of the highest efficiencies in energy conversion, which is performed without noise and vibration. Depending upon the class of fuel cell, this conversion has the potentiality to originate only water and heat as reaction products. This is done by electrochemically oxidising fuels, which are directly converted into electrical energy. On the down side, the components and the assembly of fuel cells are expensive and their life cycle is relatively short, which is associated with a loss of efficiency with time, due to the degradation of essential components, such as the catalyst or electrolyte **(Sharaf & Orhan, 2014)**. In general terms, conventional fuel cells are made up of three essential components: the electrolyte, the fuel electrode (anode) and the air electrode (cathode); depending on the fuel cell type, these basic components may differ in construction, materials and design.

Six different main fuel cell classes are described, based on the nature of the electrolyte, namely, proton exchange membrane fuel cells (PEMFC), alkaline fuel cells (AFC), direct methanol fuel cells (DMFC), phosphoric acid fuel cells (PAFC), molten carbonate fuel cells (MCFC) and solid oxide fuel cells (SOFC) **(Larminie & Dicks, 2001)**.

1.2.1. Proton exchange fuel cells

Proton exchange membranes fuel cells (PEMFC) are considered one of the most promising classes of fuel cells **(Sharaf & Orhan, 2014; C. Wang, 2004)**. PEMFCs are characterized

by the presence of a polymer, often Nafion® **(Haile, 2003)**, that guarantees permeability to protons, low electron conductivity and the physical separation between the fuel, hydrogen, present in the anode, and oxygen, present in the cathode; and a platinum (Pt)-based catalyst **(Y. Wang, Chen, Mishler, Cho, & Adroher, 2011)**. In PEMFCs hydrogen is supplied as fuel to the anode chamber, where the platinum present in the anode splits hydrogen molecules into electrons, collected by the electrode, where they are conducted to the cathode chamber, originating energy as an electric flow; and protons, that permeate through the proton exchange membrane to the cathode chamber. In the cathode chamber, the electrons and the protons are combined with atmospheric O_2, originating water and heat as reaction products, and electricity **(Haile, 2003; Sharaf & Orhan, 2014)**, as schematized in Figure 1. Due to its flexibility and scalability, PEMFCs are used in stationary, transportable and portable applications, meaning that PEMFC can function as large scale, hydrogen-based central power stations for electricity production, as powertrain for electric vehicles, such as buses, cars or motorcycles or as power supply to laptops and mobile phones **(Y. Wang *et al.*, 2011)**. Additionally, PEMFCs have low operating temperatures (60-80 ºC) **(Sharaf & Orhan, 2014)**, high power densities, excellent dynamic characteristics, when compared with other fuel cells types **(Y. Wang et al., 2011)**, are easy and safe to handle and have short start-up times **(Sharaf & Orhan, 2014)**. On the down side, PEMFCs are expensive, mainly due to the platinum-based catalyst and to the proton exchange membrane-electrode assembly and have a low durability, due to a notable degradation and loss of efficiency of the proton exchange membrane **(Sharaf & Orhan, 2014; Y. Wang *et al.*, 2011)**.

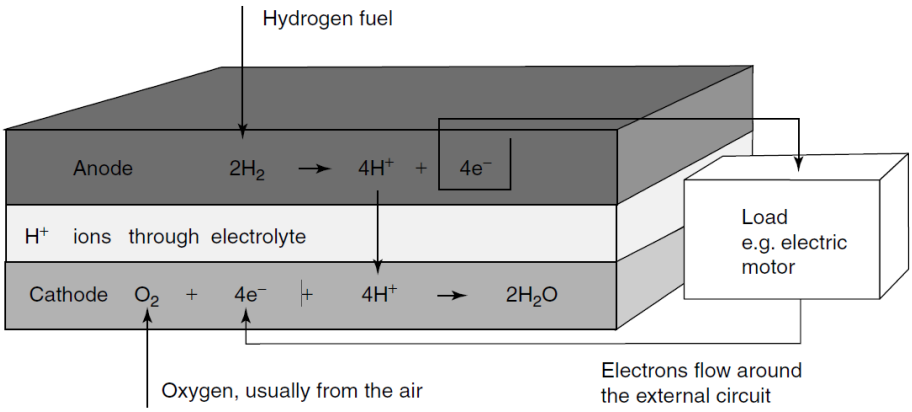

Figure 1 – General scheme of a PEMFC. Adapted from Larminie & Dicks, 2001.

1.2.2. Alkaline fuel cells

Alkaline fuel cells (AFC) are characterized by the use of alkaline electrolytes, often with solutions of potassium or sodium hydroxides. Unlike many other classes of fuel cells, AFC have OH^- as mobile ions, hence the terminology of anion exchange membranes (AEM) is often applied to the electrolytes of this class of fuel cell. Also, AFCs typical catalyst is nickel (Ni) or nickel derived, whereas in other fuel cell they are usually based on precious metals, namely platinum. AFC are described as having some of the best fuel cell performances, with conversion efficiencies around 60 to 70%, which are achieved when operating with pure hydrogen and oxygen, as fuel and final oxidant, respectively. Also, AFCs are functional in a wide range of temperatures, from below zero to 230 ºC, and of pressures, from atmospheric pressures to the vacuum of space **(Sharaf & Orhan, 2014)**. Despite this, AFCs are susceptible to the presence of impurities in both the fuel and oxidant, namely carbon oxides (CO_x) that react with the hydroxides of the electrolyte, originating carbonates and impairing the fuel cell overall performance. Additionally, the corrosive nature of the electrolyte, and the high reactant purity required, made AFCs hard and even dangerous to build and maintain, which associated with a short life time has limited almost completely the use of AFCs to space applications, namely in powering spaceships **(Larminie & Dicks, 2001; Sharaf & Orhan, 2014)**.

1.2.3. Direct methanol fuel cells

Direct methanol fuel cells (DMFC) differ from the previously discussed fuel cell classes in the way that methanol is directly used as fuel, and not hydrogen. Otherwise, some of DMFC features are similar of those of PEMFCs, including the type of proton exchange membrane, often Nafion®, and H^+ as the mobile ion **(Larminie & Dicks, 2001)**. To note that DMFC belong to a broader fuel cell class generally described as direct-fuelled fuel cells (DFFC) to which, as example, direct ethanol fuel cells, also belong **(Waidhas, Drenckhahn, Preidel, & Landes, 1996)**. DMFCs anode catalysts are made of platinum-ruthenium composites, which are optimised for the complex kinetic nature of methanol conversion to CO_2, in the anode, **(Kamarudin, Achmad, & Daud, 2009)**; this kinetics are slow and responsible for the DMFC low performances, current densities and voltages, **(Larminie & Dicks, 2001; Sharaf & Orhan, 2014)**. DMFC operational temperatures range from ambient to 110 ºC and the electrical conversion efficiencies between 35-63%

(Sharaf & Orhan, 2014). Compared with the hydrogen-based fuel cell, DMFC have the advantage of not requiring complex hydrogen production, storage and distribution systems, to which is added the fact that methanol is liquid at ambient temperatures, not only facilitating fuel management, but also increasing the potential of DMFCs for portable and mobile applications in a market traditionally dominated by lithium-based batteries **(Kamarudin *et al*., 2009)**. DMFCs show, nevertheless, many disadvantages, ranging from technological lack of optimization, (*e.g*., high catalyst loading, high cost) to CO_2 emissions and to the corrosive and toxic nature of methanol and methanol vapours, respectively **(Sharaf & Orhan, 2014)**.

1.2.4. Phosphoric acid fuel cells

Phosphoric acid fuel cells (PAFC), the most commercially developed class of fuel cells are classified as so due to the nature of the proton exchange membrane, made of phosphoric acid (H_3PO_4) in a matrix of silicone carbonite **(Sharaf & Orhan, 2014)**. As a liquid electrolyte, phosphoric acid is permeable to protons, shows thermal, chemical and electrochemical stability, is resistant to CO_2 contamination (unlike AFC's liquid electrolyte) and has low volatility **(Larminie & Dicks, 2001)**. Hydrogen is the fuel for PAFCs and H^+ the mobile ion and, as so, platinum is the catalyst used in both anode and cathode. PAFC operate at moderate temperatures, from 166 to 220 ºC, requiring an auxiliary cooling system that generally is used in cogeneration, thus increasing the fuel cell efficiency **(Xiaohang Chen, Wang, Zhao, & Zhou, 2016; Sharaf & Orhan, 2014)**. PAFC are among the most developed, more reliable and mature fuel cell technologies. Despite this, PAFCs low power densities, large size, need for auxiliary systems and slow start-up times, limit their applications to stationary household power generators **(Sharaf & Orhan, 2014)**.

1.2.5. Molten carbonate fuel cells

Molten carbonate fuel cells (MCFC) are high temperature fuel cells that use a mixture of molten lithium, sodium and potassium carbonates (Li_2CO_3, Na_2CO_3 and K_2CO_3, respectively), permeable to carbonate ions (CO_3^{2-}), in a lithium aluminium oxide ($LiAlO_2$) ceramic matrix as electrolyte **(Sharaf & Orhan, 2014)**. At the anode, the input of hydrogen reduces CO_3^{2-}ions in the electrolyte, forming CO_2 and releasing two electrons.

The produced CO_2 is subsequently transported to the cathode. At the cathode, new CO_3^{2-} ions are formed by combining CO_2 from the anode and atmospheric O_2 with the two electrons from the external circuit, thus closing the chemical and electrical cycles **(Zhang, Chen, Xu, & Ni, 2016)**. Unlike other classes of fuel cells, MCFC may operate with different fuels, such as hydrogen and methane. Due to the high operating temperatures (600 to 700 ºC), MCFCs do not require precious metals (*e.g.*, platinum) as catalysts, instead, nickel-based materials are used in both anode and cathode **(Larminie & Dicks, 2001)**, also allowing for the use of MCFC in combined heat and power systems ***(Zhang et al.*, 2016)**, thus achieving the highest reported efficiencies in methane-electric energy conversion, 55 to 65% **(Sharaf & Orhan, 2014)**. Nevertheless, MCFCs have some disadvantages, namely, slow start-up times, low power densities and a corrosive electrolyte that limits the fuel cell life cycle by degrading metallic parts and dissolving the catalyst. MCFCs are applied mainly in stationary electricity generating systems **(Pachauri & Chauhan, 2015; Sharaf & Orhan, 2014)**.

1.2.6. Solid oxide fuel cells

Solid oxide fuel cells (SOFC) use an oxide ion-conductor ceramic material as electrolyte. This electrolyte is of zirconia (ZrO_2) stabilized by yttria (Y_2O_3) that conducts O^{2-} ions. Due to the high operating temperatures (600 to 1000 ºC), SOFC do not require expensive catalysts, indeed, the anode is made of a metallic nickel cement and the cathode of strontium-doped lanthanum manganite, a semi-conductor **(Larminie & Dicks, 2001; Mehmeti, McPhail, Pumiglia, & Carlini, 2016)**. The solid nature of SOFC, and the fact that, due to the high temperatures, the fuels are in gas form, makes this fuel cell class the simplest **(Larminie & Dicks, 2001; Minh, 2004)** and highly reliable, if operating continuously **(Haile, 2003)**. SOFCs have high fuel flexibility, and show energy conversion efficiencies around 55-65%, that can increase up to 90% when operating with combined heat and power cycles **(Mehmeti *et al.*, 2016; Sharaf & Orhan, 2014)**. SOFC are mainly applied in stationary and transportation systems and their limitations are associated with low power densities, slow start-up times and durability issues, originated by thermal stresses in structural components **(Sharaf & Orhan, 2014)**.

1.3. Microbial fuel cells

Microbial fuel cells (MFC) are devices that use active microorganisms as biocatalyst to produce electricity from organic matter. Generically, MFCs are made of an anoxic anode chamber and a cathode chamber, physically separated by an ionic exchange membrane, plus the necessary operational wiring and piping. In the anode chamber, microorganisms oxidize an organic substrate, originating electrons, protons and carbon dioxide. Protons are conducted through the proton exchange membrane (PEM) to the cathode chamber, where they react with electrons, conducted through an external electric circuit, and reduce atmospheric oxygen to water. The external flow of electrons is responsible for the electric energy production **(Rahimnejad *et al*., 2015)** and is only generated due to the absence of a natural electron acceptor, such as oxygen or nitrogen, which is substituted by the MFC anode **(Rabaey & Verstraete, 2005)**. In a MFC, the organic substrate must be continually or cyclically replenished, otherwise, the device is considered to be a bio-battery **(Logan *et al*., 2006)**.

1.3.2. Design and components

The dual-chamber design (Figure 2a), requires an anoxic anode chamber where anaerobic microorganisms oxidize an organic substrate, originating CO_2, protons and electrons; a PEM, that conducts protons and prevents the diffusion of O_2 to the anode chamber; and a cathode chamber, where atmospheric O_2 is reduced, in the cathode, to water by the presence of electrons and protons **(Rahimnejad *et al*., 2015)**. Despite this, other configurations have been tested, such as the single-chamber MFC (Figure 2b) attempting to develop a simpler, cheaper and easier to scale-up system, where the cathode is directly exposed to air **(Du, Li, & Gu, 2007; Liu Hong, 2004)**.

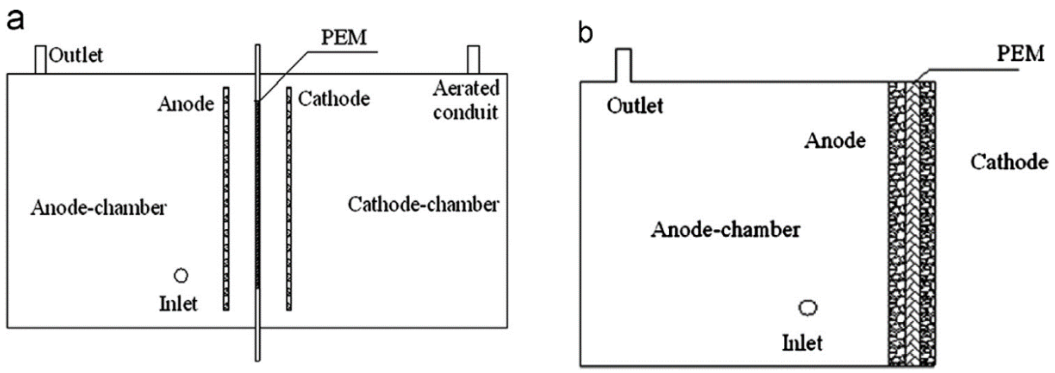

Figure 2 – General configurations of a double-chamber MFC, a, and single-chamber MFC, b. Adapted from Leong *et al*., 2013.

1.3.2.1. Anode

In a MFC, the anode function is to serve as physical support for the microorganisms to grow on, and to facilitate anodic microbial electron transfer; for this, the anode material must have good electric conductivity, low resistance, biocompatibility, chemical stability, high surface area and mechanical strength. Most anodes are made of carbon derived materials, namely graphite, in various geometrical arrangements, such as graphite rods, granules, cloth, fibres or carbon paper **(Rahimnejad *et al*., 2015)**. In order to improve MFC output, nanomaterials, such as carbon nanotubes, and conducting composites of organic polymers, such as poly(tetrafluoroethylene) (PTFE) and polyaniline, and modified carbon or metals were used as base materials for the anode **(Dutta & Kundu, 2014; Rahimnejad *et al*., 2015)**.

1.3.2.2. Cathode

The cathode mediates the electron transfer from the external MFC electrical circuit to the cathodic chamber, where they reduce the final electron acceptor, which usually is O_2, due to its high oxidation potential, availability, and sustainability **(Logan *et al*., 2006)**. Despite this, ferricyanide is also used, mainly at the experimental level, for its good performance when working with a carbon cathode. Ferricyanide needs, however, to be replaced when all ferricyanide is converted to ferrocyanide (oxidised form), and also impairs the MFC long term performance by diffusing into the anodic chamber **(Logan *et al*., 2006; Rahimnejad *et al*., 2015)**. As already referred, cathodes may be made of carbon (*e.g*. graphite), but this solution has very slow kinetics and large over potentials in O_2 reduction. The use of

platinum catalysts increases the fuel cell performance, as well as other compounds, such as ferric (Fe^{3+}) and cobalt (Co) complexes and manganese oxide **(Dutta & Kundu, 2014)**. Also, as an alternative to catalysis by oxygen oxidation, bio-cathodes have been tested, where the cathodic reactions are catalysed by microorganisms, without the need for abiotic catalysis or the addiction of artificial electron mediators. Bio-cathodes are generally described as enhancers of cathode performance and to improve MFC electrical production. Depending on the final electron acceptors, bio-cathodes can be anaerobic (*e.g.*, nitrate and sulphate) or aerobic (O_2) **(Milner *et al*., 2016; Rahimnejad *et al*., 2015)**.

1.3.2.3. Proton exchange membrane

The PEM is one of the critical components of the MFC conventional design and has a significant impact in MFCs overall cost and performance **(Leong *et al*., 2013; Rahimnejad *et al*., 2015**). In general terms, PEM function is to enable the transport of protons from the anodic to the cathodic chamber, whilst preventing O_2 diffusion to the anodic chamber and substrate crossover to the cathodic chamber. PEM have negatively charged functional groups attached to the membrane matrix, thus allowing the transport of protons (as well as other positively charged ions) through the electrolyte, by diffusion, accordingly with the concentration differential **(Rahimnejad *et al*., 2015)**. PEM resistance to proton crossover is one of the critical PEM characteristics, determining MFC power and current densities **(Leong *et al*., 2013)**.

Nafion® is the most popular PEM for MFC applications, due to its high proton conductivity, originated by the negatively charged hydrophilic sulfonate groups. Nafion® is described as having some of MFCs best performances **(Leong *et al*., 2013)**, notwithstanding, its high costs (about 38% of MFC total capital cost) **(ElMekawy, Hegab, Dominguez-Benetton, & Pant, 2013)** lead to the application of several alternative PEMs in MFCs, such as Ultrex®, Hyflon® or Zirfon®.

Some specific problems arise with the use of PEMs in MFC, namely biofouling, pH splitting or O_2 diffusion. Biofouling, the growth of biofilms on the membrane surface is a phenomenon that lowers both the transport rate of protons and the crossover of organic substrate to the cathodic chamber and which influence can be diminished by the development of anti-adhesion or anti-microbial techniques. pH splitting, a difference of pH on the anodic and cathodic chambers can drastically affect the MFC performance. This

occurs due to a competition for attachment with the PEM negatively charged sites with other cations present in solution (*e.g.* Na^+, K^+, Ca^{2+}, Mg^{2+} and NH^{4+}), reducing proton transport. pH splitting problems can be eliminated with the use of AEM that employ OH^- as mobile ion. O_2 diffusion to the anodic chamber impairs MFC performance, by competing with the anode as a more favourable electron acceptor **(Leong *et al*., 2013)**.

The subject of the PEM for more generic fuel cell applications will be approached with more detail in the section 1.4 of this work.

1.3.3. Microorganisms used in MFC

Microorganisms have the ability to produce electrons from the metabolization of organic substrates. In a MFC, microorganisms are separated from the final electron acceptor so that electron transference to the MFCs anode is the only mean to restore intercellular electron mediators and complete respiration, hence originating electric current **(Logan & Regan, 2006)**.

1.3.3.1. Bioelectrogenesis

The microorganism's metabolic activities, either anabolism or catabolism, occur in the presence or absence of O_2, thus describing the two major classes of microbial metabolism, aerobic or anaerobic, respectively. Despite the class of microbial metabolism, microorganisms oxidise the available substrate, creating reducing equivalents, protons and electrons, in the form of redox carriers such as nicotinamide adenine dinucleotide (NAD^+), flavin adenine dinucleotide (FAD^+) or flavin mononucleotide (FMN^+), among others. These carriers are essential in the generation of energy in the form of adenosine triphosphate (ATP) during respiration. In anaerobic conditions, reducing equivalents move through the electron transport chain until reaching a terminal electron acceptor. Concomitantly, a proton motive force is generated that assists in creating energy in the form of ATP. The terminal electron acceptor is determined upon the availability of the most thermodynamically suited compound, that is, the one with the higher reduction potential. In the presence of O_2, that has the highest reduction potential in biological systems, as well as being strongly electronegative, the reducing equivalents reduce O_2 to water. In the absence of O_2, other compounds assume the function of terminal electron acceptor. Therefore, in anaerobic conditions, this electrical potential can be harnessed by

the introduction of an artificial terminal electron acceptor **(Mohan, Velvizhi, Modestra, & Srikanth, 2014)**.

In a MFC, the anode artificially collects the produced electrons, assuming the terminal electron acceptor function in the anodic chamber and assuring the conditions for the microorganisms to maintain their biological functions by recuperating the redox potentials of intracellular mediators without a chemical terminal electron acceptor (*e.g.*, O_2, nitrates or sulphates) **(Mohan *et al.*, 2014)**. In a MFC, the anode potential has an influence in the microorganism metabolism. With the decrease of the anode potential, the microorganisms are forced to deliver electrons through more reduced complexes, which will determine the redox potential of the final electron shuttle and, consequently, the microorganism's metabolism. If the anode potential decreases in the presence of alternative terminal electron acceptors, such as sulphate or nitrate, microorganisms will transfer electrons to these compounds, lowering the MFC performance. Depending on the anode potential, microorganisms may assume high, medium or low redox oxidative metabolisms or fermentation **(Rabaey & Verstraete, 2005)**.

1.3.3.2. Anodic electron transfer

One of the critical features in the MFC performance, in what is directly related with the microorganisms' nature and/or metabolism, is the electronic transference from the cells to the MFC's anode, one of the limiting factors of MFC performance. The intracellular electrons produced by the organic substrate oxidation are transferred either by direct electron transfer (DET) or by mediated electron transfer (MET), as shown in Figure 3. Both this transfer systems depend, up to a certain extent, on membrane permeability for the establishment of transmembrane proteins, that facilitate the transport of electrons or for the transport of electron carriers **(Mohan *et al.*, 2014)**. The natural occurrence of electric transference phenomena in many bacterial communities (*e.g.* biofilms) is indicative of the biological relevance of this process in inter-bacteria communication and in quorum sensing processes **(Logan, 2009; Mohan *et al.*, 2014)**.

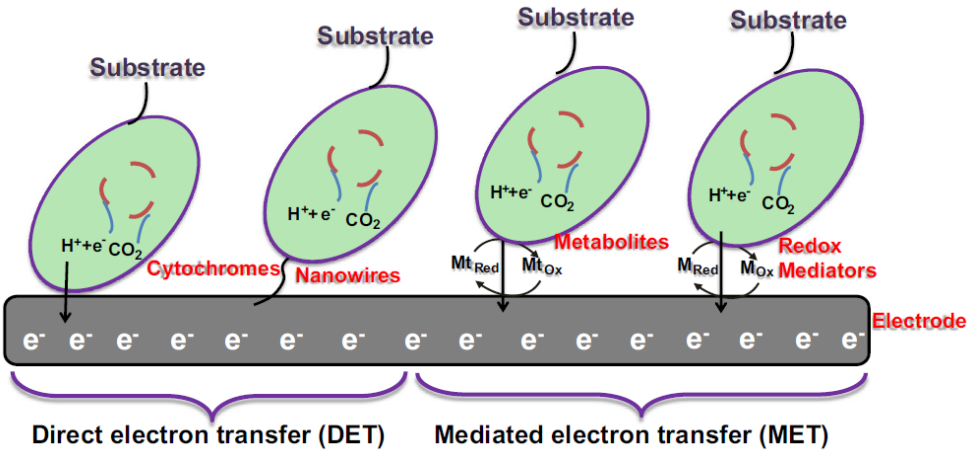

Figure 3 – Transference of electrons from bacteria to the anode can be performed directly, by DET (through membrane proteins or nanowires), or indirectly, by MET (through chemical mediators). Adapted from Rahimnejad *et al.*, 2015.

For DET to occur, the microorganisms need to be in physical contact with the anode's surface. This contact can either be established by trans-membrane proteins or by conductive pili known as nanowires. Membrane c-type cytochrome and multi-heme proteins are identified as potentially performing DET. The disadvantage of this membrane protein-mediated transference is bound with the fact that only the first biofilm layer, the one directly in contact with the anode, can perform DET, leaving unexplored most of the biofilm bioelectric potential. On the contrary, nanowire-mediated DET allows the formation of tick electroactive biofilms, with the establishment of a bacteria-to-bacteria and bacteria-to-anode network of electron conducing nanowires, described to increase anode performance **(Schneider, Kovács, Rákhely, & Czeller, 2016; Mohan *et al.*, 2014)**.

MET occurs when electron transference is mediated by shuttles that are reduced by electrons within the cell membrane and become oxidised in contact with the anode, usually being able to perform this process cyclically. A critical factor in MET is membrane permeability, indeed, MET rate is described to increase with the addition of membrane permeabilizers (*e.g.*, chitosan, ethylenediaminetetraacetic acid and polyethyleneimine) or with the heterologous expression of porin proteins **(Mohan *et al.*, 2014)**. Electron mediators may be artificially added to the culture (*e.g.*, neutral red, thionin or methyl viologen) **(Rabaey & Verstraete, 2005)** or be primary or secondary soluble metabolites endogenously produced by MFC cultures, such as flavins and phenazines **(Schröder, Harnisch, & Angenent, 2015; Mohan *et al.*, 2014)**.

1.3.3.3. Microbial communities in MFC

MFC operate mostly with bacteria, though there are works where yeasts were applied in energy production **(Raghavulu, Goud, Sarma, & Mohan, 2011)**. The cultures used in MFC can either be pure bacterial monocultures or mixed cultures, however, mixed cultures are often referred as producing higher MFC performances **(Logan, 2009)**. This communities are originated from environmental samples, such as waste waters, sludge, sediments or purpose bioreactors and are frequently naturally electroactive **(Logan, 2009; Logan *et al.*, 2006; Mohan *et al.*, 2014)**. Despite the microorganism's importance for MFC operation, characteristics associated with fuel cell architecture and components, electrode spacing and solution conductivity are often more significant for the final fuel cell performance than the microorganism nature **(Logan, 2009)**.

In MFC operation, pure cultures or bacterial isolates are mostly used in laboratory scale, for research purposes. *Geobacter sulfurreducens*, *Rhodoferax ferrireducens*, *Aeromonas hydrophila*, *Pseudomonas aeruginosa*, *Pseudomonas otitidis*, *Geopsychronacter electrodiphilus*, *Desulfobulbus propionicus*, *Escherichia coli*, *Rhodopseudomonas palustris* DX-1, *Shewanella oneidensis* and *Shewanella haliotis* are some of the bacterial species and strains that were tested and found to be electrochemically active **(Mohan *et al.*, 2014)**. These microorganisms also produce nanowires, increasing anode-microorganism contact and MFC power density. Among this referred to species, *Geobacter* and *Shewanella* are the most studied genera. While operating MFCs with pure cultures, concerns with the maintenance of sterile conditions and the requirement for pure substrates are two of the major drawbacks **(Mohan *et al.*, 2014)**. Notably, 51% of the published studies concern MFC operation with pure cultures **(Mercuri, Kumata, Amaral, & Vitule, 2016)**.

MFCs operated with mixed cultures are typically open systems more focused on the industrial applications of waste water treatment/energy production **(Mohan *et al.*, 2014)**. The nature and composition of this communities varies accordingly with the type and availability of the substrate **(Sotres, Tey, Bonmatí, & Viñas, 2016; Mohan *et al.*, 2014)**, inoculum origin, reactor design and operational conditions. Despite higher power densities, MFC operated with mixed cultures, habitually show lower Columbic efficiencies due to complex metabolic reactions and mass transfer losses **(Mohan *et al.*, 2014)**. 34% of the published studies deal with MFC operation with mixed cultures **(Mercuri *et al.*, 2016)**.

1.3.4. Operational parameters

1.3.4.1. Temperature

MFCs are strongly affected by temperature alterations, due to its influence in process kinetics, mass transfer, thermodynamics and in the nature and distribution of the microbial communities. Regarding MFC performance, temperature is important to both power output and organic matter removal, and, generally, is higher as temperature increases. Higher temperatures also reduce fuel cell ohmic resistance and, thus, internal resistance, which can explain an increase in ionic conductivity. To note that the referred temperature increase is in the 30 to 45 ºC threshold, where biofilms have their maximum bio-electrocatalytic activity. Regarding the MFC start-up process, in which the influence of temperature is critical, higher initial temperatures are described to increase MFC performance, even if the long term operation is performed under lower temperatures **(Oliveira, Simões, Melo, & Pinto, 2013)**.

1.3.4.2. pH

pH constrains MFC operation in the way that it influences both the physiology of microorganisms and many of the fundamental process that regulate MFC operation, such as proton transport in PEM. Biologically, external pH fluctuations influence cytosolic pH, ion concentrations, membrane potentials and proton shuttling, not to mention the impact of pH in bacterial growth **(Mohan *et al.*, 2014)**. Continuous MFC operation leads to an accumulation of protons in the anodic chamber which decreases pH in this compartment, due to PEMs slow or inefficient proton transport. Concurrently, in the cathodic chamber, O_2 reduction decreases proton concentration, increasing pH, in process known as pH splitting **(Leong *et al.*, 2013)**.

Anodic chamber pH microenvironment is, thus, of critical importance, influencing bacterial metabolic activity, substrate oxidation and proton and electron production mechanisms. Once near-neutral conditions are optimal for bacterial growth, buffer systems are sometimes applied. An ideal buffer system for MFC should maintain pH constant, whereas facilitating proton transport, without interfering with bacterial activity or chemical reactions. Despite this, the use of chemical buffer systems is not practical for real MFC

applications, for it is associated with increasing cost and energy input **(Oliveira *et al*., 2013)**.

Generally, acidophilic operations are responsible for better MFC performances, if compared with neutral or alkaline operation, because of possible acidogenic pathways and higher cell proton gradient **(Mohan *et al*., 2014)**.

1.3.4.3. Organic substrate

The type, nature and concentration of organic substrate utilized in a MFC influences the microorganism community and, hence, the fuel cell overall performance **(Mohan *et al*., 2014)**. Diverse substrates have been utilized in MFC operation, generally classified as natural (*e.g*., gross domestic water, lactate, marine sediment, sewage sludge), or synthetic/ pure substrates (*e.g*., industrial wastewater, ethanol, glutamate, propionate, fumarate, acetate) **(Mercuri *et al*., 2016)**. In general, complex waste waters are hard to metabolize due to long carbon chains and aromatic rings. Simple substrates originate many reducing equivalents, enhancing MFC performance. Wastewaters from industries or domestic activities are also considered good substrates, due to high quantities of degradable organic and fermentable solid products, such as the wastes from agriculture and human alimentation. Besides the influence on the microorganisms, the substrate organic load also influences fuel cell power densities and Coulombic efficiencies **(Mohan *et al*., 2014)**.

1.3.5. MFC applications

The basic mode of operation and the process nature of MFCs are primarily conceptualized for wastewater treatment with simultaneous electricity production. Despite this, minor changes in MFC operation may expand the operational focus to bio-hydrogen production and biosensor applications **(Rahimnejad *et al*., 2015)**.

Domestic wastewater contains more energy (about nine times more) than the amount that is needed to treat it through intensive aeration process, whereas the use of MFCs produces energy and yields a lower amount of sludge than the aeration process **(Logan, 2009)**. In this regard, MFCs can be used to treat wastewater from various human activities, such as sanitary washes, food processing wastewaters or swine wastewaters, all rich in organic compounds, of which up to 90% of chemical oxygen demand (COD) can be removed. However, MFC bioelectricity production is still relatively low and more suited to

sustainable long-term power applications **(Rahimnejad *et al*., 2015)** or to remote power supply applications, where traditional power deliver systems, such as batteries, are not feasible **(Logan, 2009)**. Additionally, compared with traditional methods, MFC wastewater treatment has a small environmental footprint and higher operational stability **(Mercuri *et al*., 2016)**.

MFC operation can be readily adapted to bio-hydrogen instead of electricity production, for this, the anode potential has to be increased, by voltage application and the cathode has to be deprived from O_2 **(Rahimnejad *et al*., 2015)**.

The bio-sensoric application of MFC can be harnessed for biological contamination determination or toxic compound activity detection. In the first case, a sterile fuel cell detects contamination by microorganisms by generating electricity when the microorganism establishes contact with the cell and produces energy. The presence of toxic compounds can be detected by a decrease in the power output of a MFC operated by a sensitive species **(Schneider *et al*., 2016)**.

Another MFC application is in the remediation of soils contaminated by toxic metals, such as lead (Pb) or cadmium (Cd). In this field, MFC application is described to be feasible but not as effective as electrokinetic soil remediation, despite the advantage that with MFC mediated soil remediation the input of electricity is not required **(Habibul, Hu, & Sheng, 2016)**.

The interest in MFC research and development has increased in the last years, indeed, 84.7% of MFC-related studies were published between 2006 and 2014 **(Mercuri *et al.*, 2016)**. The existence of studies comparing the efficiency of MFC electricity production *versus* the cost of critical MFC components (*e.g*. Stoll, Ma, Trivedi, Spear, & Xu, 2016) even with the sacrifice of performance, in order to determine cost-effective alternatives and the economical reliability of MFC operation is the evidence of MFC potentiality and general interest. Nevertheless, the main technological barrier for MFC wide application is the scale, still confined to small prototypes that are insufficient to produce electricity for practical proposes **(Mercuri *et al*., 2016)**.

1.3.6. Limitations of MFC performance

A theoretical approach determined the maximum possible power density in 16.000 kW *per* fuel cell m^3, based solely on the bacterial electrical potential **(Logan, 2009)**. The fact that

these densities are not obtained is described as the responsibility of bottlenecks associated with cell architecture, component materials and several overpotentials. These overpotentials are discriminated as activation overpotentials, linked with the activation energy required for substrate oxidation on the anode or with O_2 reduction on the cathode; related with concentration polarizations, when compounds are being oxidized faster than their transport, leading to accumulations; and concerning ohmic losses, induced by electrical resistance of electrodes and electrolyte and low PEM conductivity **(ElMekawy *et al.*, 2013)**.

1.4. Proton exchange membranes

An ideal PEM should have high proton conductivity (superior to 0.01 S cm^{-1}) and low fuel permeability, as well as thermal, dimensional and hydrolytic stability. The first membranes to draw attention towards PEM development were perfluorosulphonic ionomer (PFSI) membranes, which were attractive due to their high proton conductivity and stability when exposed to oxidative or reductive environments **(Bakangura, Wu, Ge, Yang, & Xu, 2015)**. In PFSI membranes, proton conductivity is thought to occur due to the combined morphology of tetrafluoroethylene hydrophobic backbones and side chain hydrophilic-terminated sulphonic groups. When hydrated, the sulphonic groups form ionic clusters that create wide well-connected hydrophilic channels, allowing proton transport. PFSI membranes possess serious drawbacks, such as poor proton conductivity above 80 ºC, high production costs **(Bakangura *et al.*, 2015)** and environmental problems **(Gadim *et al.*, 2015)**. Additionally, PFSI membranes proton conductivity performance depends heavily in the membrane hydration levels, as well as the mechanical properties **(Hickner *et al.*, 2004)**. Notwithstanding, on MFC, the PEMs are always highly hydrated.

1.4.2. Proton conducting mechanisms

In solution, protons do not exist as isolated protons, but rather as hydrated proton molecules, namely as H_5O^{2+} dihydronium ion complex or as $H_9O_4^+$ complex. The high proton conductivity in water is attributed to the exchange of protons along water molecules in contact by hydrogen bridges, known as proton wires. Protons propagate along a proton

wire, meaning that a proton leaving a proton wire is not the same that has entered it in the first place **(Buch-Pedersen, Pedersen, Veierskov, Nissen, & Palmgren, 2009)**.

In hydrated polymeric matrixes, proton transport is described by two principal mechanisms, the "proton hopping" and the vehicular mechanisms where water functions as vehicle for proton transport (Figure 4) **(Kim *et al.*, 2015; Peighambardoust, Rowshanzamir, & Amjadi, 2010)**.

According to the proton hopping mechanism, also known as structural diffusion, protons are transferred from one hydrolysed ionic site, such as SO_3^- or H_3O^+, to another across the membrane. **(Peighambardoust *et al.*, 2010)**. When plotted in an Arrhenius plot, the proton conductivity, if behaving according with this mechanism, follows the Vogel-Tamman-Fulcher (VTF) model, that describes the behaviour of protons at higher temperatures or lower relative humidity (RH). According with this model, the movement and flexibility of the membrane polymer, dependent of the glass transition temperature, has a great importance in proton hopping in long ranges **(Di, Piga, Giffin, & Pace, 2012; Gadim *et al.*, 2017; Giffin *et al.*, 2012)**.

By the vehicular proton transport mechanism, hydrated protons (hydronium ions), diffuse through the membrane aqueous medium according with the electrochemical gradient. For this it is essential the existence of free water volumes in the matrix **(Kim *et al.*, 2015)**, which are created by the hydrophobic nature of the hydrated membrane polymer backbone **(Peighambardoust *et al.*, 2010)** in synergy with the hydrophilic side chain sulphonic groups **(Bakangura *et al.*, 2015)**. This transport mechanism follows the Arrhenius model, that describes the proton behaviour for membranes in conditions of lower temperatures and higher RH associated with lower polymer flexibility **(Di *et al.*, 2012; Gadim *et al.*, 2017)**.

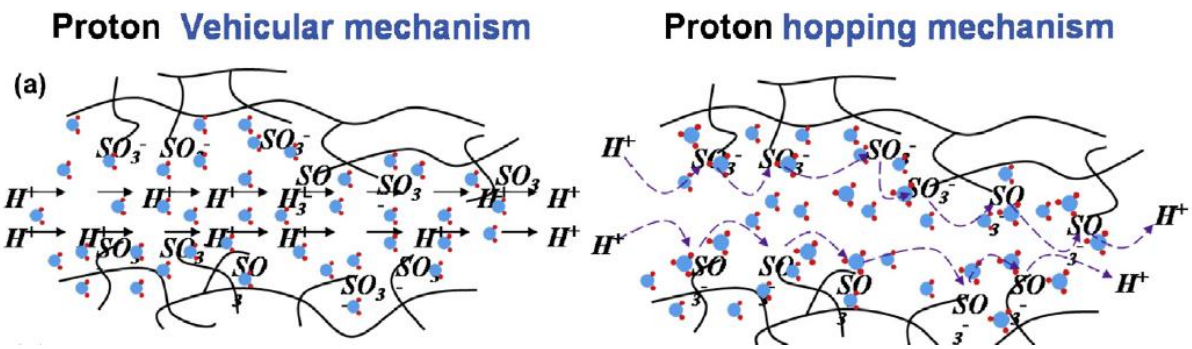

Figure 4 – Proton vehicular and hopping mechanisms in a hydrated PFSI membrane. Adapted from Kim *et al*., 2015.

1.4.3. PEM matrix polymers

The polymer chemical structure has a significant influence in the membrane properties. Therefore, polymer polarity, glass transition temperature, thermal stability and solubility are very important characteristics **(Bakangura *et al*., 2015)**. For PEM applications, glassy thermoplastic polymers are mostly used, due to their excellent film-forming abilities, dynamic flexibility and thermal stability. Non-conducting polymers require the attachment of protogenic groups to the polymer chain. PFSI polymers exhibit excellent electrochemical properties and chemical stability but their high cost lead to the development of polymers with fluorite-free structures **(Bakangura *et al*., 2015)**.

1.4.3.1. Fluorinated polymers

Fluorocarbon polymer based PEM, due to the fluorite small size and high electronegativity have strong C–F bonds and low polarizability **(Peighambardoust *et al*., 2010)**. These polymers show high thermal stability, chemical inertness and proton conductivity **(Kim *et al*., 2015; Peighambardoust *et al*., 2010)**, attributed to the high PTFE backbone acidity as well as to the side chain sulphonic groups. PFSI membranes form uniform and effective water channels, showing good electric properties, despite the low water uptake. These membranes are the most used for PEMFC applications, being, however, hard and costly to prepare and assemble. The most used PFSI PEM is Nafion®, despite the existence of similar polymeric alternatives, such as Aciplex™, Flemion™ and Fumapem®, produced by diverse companies **(Kim *et al*., 2015)**.

1.4.3.2. Non-fluorinated polymers

The drawbacks of PSFI membranes lead to the development of alternative solutions for PEM production, among which are the non-fluorinated polymers **(Bakangura *et al*., 2015)**. These can be aliphatic or aromatic polymers, with the latter having benzene ring structures in the polymer backbone or side chains **(Peighambardoust *et al*., 2010)** that allow the hydrocarbon membranes to be easily designed according with predetermined properties. Additionally, the monomers are cheaper than PSFI **(Kim *et al*., 2015)** and

easily recycled by conventional methods. Generally, hydrocarbon polymers with polar groups have high water uptake capacity over a wide range of temperatures **(Kim *et al.*, 2015; Peighambardoust *et al.*, 2010)**, with water channel formation and enhanced proton conductivity and also showing elevated thermal and mechanical stability. However, non-fluorinated hydrocarbon membranes have lower oxidative and chemical stability, when compared with fluorinated ones **(Kim *et al.*, 2015)** though some of this differences may not relevant on the context of MFC operation. Some of the most relevant hydrocarbon polymers for PEM applications are polyether sulphones, polyether ketones, polyesters and poly(arylene ethers) **(Kim *et al.*, 2015; Peighambardoust *et al.*, 2010)**.

1.5. Bacterial cellulose

Cellulose is the most abundant natural polymer, being estimated that 10^{11} to 10^{12} tonnes of cellulose are produced by photosynthesis every year. Cellulose may derive from various sources, namely from wood, seed fibres (*e.g.*, cotton, coir), bast fibres (*e.g.*, flax, hemp), grasses (*e.g.*, bagasse, bamboo), marine animals (*e.g.*, tunicate), algae, fungi, invertebrates and bacteria. Wood is the most significant source of industrial cellulose, where it is found associated with hemicelluloses, lignin, extractives and inorganic salts **(Nechyporchuk *et al.*, 2015**).

At the molecular level, cellulose is a linear homopolymer of D-glucose units, covalently linked by $\beta(1\rightarrow4)$ glycosidic bonds that leads to a flat conformation (Figure 5). This arrangement allows the formation of intra- and inter-molecular hydrogen bonds, responsible for cellulose crystallinity and mechanical properties **(Panaitescu, Frone, & Chiulan, 2015)**. The cellulose polymer repeat unit, known as cellobiose units, comprises two anhydrous glucose rings, as shown between brackets in Figure 5 **(Eichhorn *et al.*, 2010)**. The degree of polymerization of native cellulose ranges from 10 000 to 44 000 glucose monomers, depending on the source **(Nechyporchuk *et al.*, 2015)**.

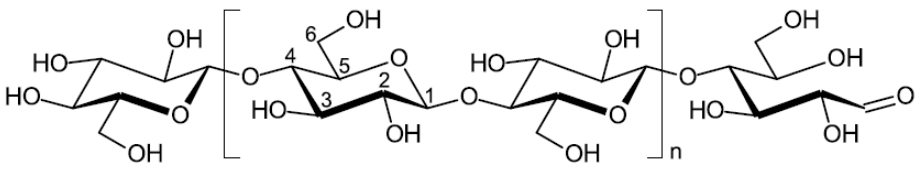

Figure 5 – Cellulose polymer, highlighting the cellobiose unit between brackets, as well as the non-reducing (left) and reducing (right) end groups. Adapted from Nechyporchuk *et al.*, 2015.

Cellulose chains are arranged in elementary fibrils that are in turn aggregated into larger microfibrils with 5 to 50 nm in diameter and several microns of length. Cellulose is considered a semi-crystalline polymer, due to the existence of both crystalline and amorphous regions in cellulose fibrils **(Moon, Martini, Nairn, Simonsen, & Youngblood, 2011)**.

The nanotechnological revolution further increased the scope of cellulose applications *via* the introduction of nanocellulosic substrates. Nanocelluloses are classified as nanofibrilated cellulose, when obtained by mechanical processes, as cellulose nanocrystals or nanowhiskers, when produced by acidic treatment, and as bacterial nanocellulose **(Panaitescu *et al.*, 2015)** when synthesized by bacteria. Nanofibrillated cellulose and cellulose nanocrystals are obtained in a top-down process by the treatment and disintegration of vegetable cellulose fibers, whilst bacterial cellulose produced in a bottom-up process by the build-up of cellulose nanofibers **(Nechyporchuk *et al.*, 2015)**.

Bacterial cellulose (BC) is a high purity cellulose produced by some aerobic bacteria in aqueous medium from sugars. BC has the same chemical structure as vegetable cellulose, though being free from other biopolymers such as hemicelluloses and lignin **(Nechyporchuk *et al.*, 2015)**. Additionally, after purification, BC has only hydroxyl functional groups, **(Klemm *et al.*, 2011; Nechyporchuk *et al.*, 2015)** unlike wood-based cellulose, that often presents carbonyl or carboxyl groups, introduced by the cellulose treatment and purification processes. BC is found in the form of twisting ribbons, with cross-sections of 3-4 nm × 70-140 nm of area and more than 2 μm in length. The BC degree of polymerization varies from 3000 to 9000 and shows a crystallinity of 80 to 90% **(Nechyporchuk *et al.*, 2015)**, while vegetable cellulose crystallinity ranges from 40 to 60% **(Cacicedo *et al.*, 2015)**.

The BC biogenesis is done by aerobic bacteria as a way to guarantee access to atmospheric O_2 and protection against UV radiation or aggressive chemical environments. BC biosynthesis follows a three-level hierarchical structure. Initially, about 16 synthetized cellulose chains are extruded from pores in the bacteria cellular wall, originating a first assembly with 1.5 nm in diameter that combines in 3 to 4 nm diameter protofibrils. These arrange in crystalline microfibrils (20 nm width), which, in turn, associate in flat cellulose

ribbons with 80 to 120 nm in diameter and length of hundreds of microns. This process is schematized in Figure 6 **(Panaitescu *et al*., 2015)**.

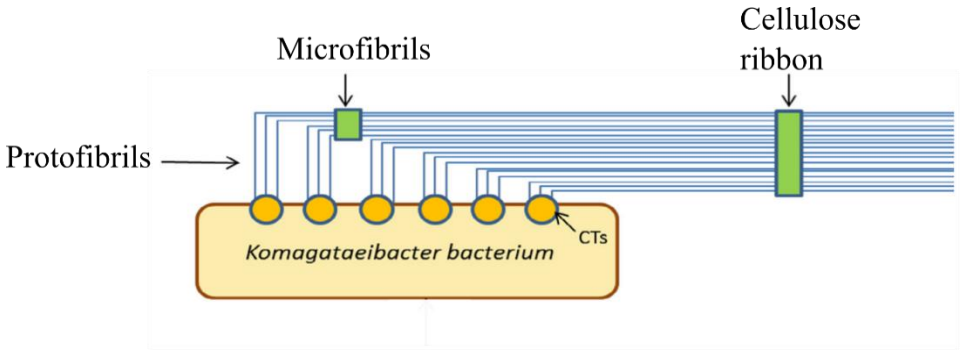

Figure 6 – Schematized process of BC production. Adapted from Cacicedo *et al*., 2015.

BC is mostly produced by bacteria found in environments where the fermentation of sugars occurs, such as damaged fruits, unpasteurized juices, beers or wines. The most relevant *genera* are *Komagataeibacter* (formerly known as *Acetobacter* and as *Gluconacetobacter* **(Yamada, 2014)**), *Sarcina*, *Agrobacterium* and *Rhizobium* **(Cacicedo *et al*., 2015)**, despite only *Komagataeibacter* sp. being able to produce BC at commercial levels and *Komagataeibacter xylinus* remaining the model strain for research and commercial purposes **(Figueiredo, Vilela, Neto, Silvestre, & Freire, 2014)**. Physiologically, the *Komagataeibacter* genus is characterized by the ability to metabolize ethanol to acetic acid, oxidate acetate and lactate to carbon dioxide and water, and to be able to grow in the presence of 0.35% (w/v) acetic acid, without the production of 2,5-diketo-D-gluconate from glucose; additionally, the *Komagataeibacter* genus is morphologically unable of mobility. The *Komagataeibacter* species are strict aerobic, Gram-negative bacteria, found predominantly in fruits and vegetables in decomposition, where they metabolize carbon sources such as glucose, fructose, sucrose, mannitol and glycerol, among others, in temperatures ranging from 25 to 30 ºC and pH of 3 to 7. The production of cellulose in the culture medium-air interface works as a fluctuation mechanism, allowing the bacteria to have simultaneous access to O_2 and nutrients, while also functioning as a physical barrier to protect the bacteria from external aggressions, increasing the ability to colonize other substrates and, due to the BC hydroscopic nature, retaining moisture, thus preventing dehydration **(Cacicedo *et al*., 2015)**.

The interest in BC as a biodegradable biopolymer has increased significantly in recent years with the development of many BC-based composites, that take advantage of

the BC unique set of characteristics as well as with the interest to develop methods to produce BC at commercial levels **(Figueiredo *et al*., 2014)**.

1.5.1. BC production

The synthesis of of BC by *K. xylinus* is a three step process: i) polymerization of glucose residues with $\beta(1\rightarrow4)$ glycosidic bonds; ii) extracellular extrusion of linear cellulose chains and, iii) organization and crystallization of cellulose microfibrils through the establishment of hydrogen bonds and van der Waals interactions **(Jozala *et al*., 2016)**. The cultivation method and conditions have a significant influence in the BC final structure and physical and mechanical properties **(Figueiredo *et al*., 2014)**. The culture medium is the most important factor to the final BC cost, which has propelled the research towards the identification of low-cost culture mediums, that could improve BC yields and economic viability **(Jozala *et al.*, 2016)**.

BC production is often performed in the Hestrin-Schramm (HS) medium that uses glucose as main carbon source. In order to find cheaper mediums, alternative carbon sources have been tested, such as xylose, maltose, starch, polyols (*e.g*., glycerol) or residues and industrial wastes (*e.g.* grape bagasse or dry olive mill residue) **(Figueiredo *et al*., 2014)**. Other strategies envision the addition of inductors to activate the microorganism energetic metabolism and/or reduce the formation of metabolic by-products **(Cacicedo *et al*., 2015)**.

Diverse fermentation dynamics have also been tested, namely, batch, fed-batch and continuous fermentations, under static or agitated conditions. However, the impact of the different dynamics in BC physical characteristics, properties and morphology must be acknowledged **(Cacicedo *et al*., 2015)**.

BC production under static conditions is the most common method, originating highly hydrated cellulose membrane (Figure 7). These membranes are originated in the culture medium-air interface where the increase in thickness forces the mature BC membrane to sink, allowing the bacteria to maintain O_2 access. With the use of shaped casts, it is possible to give predetermined forms to the membrane for specific applications **(Figueiredo *et al*., 2014)**. This method yields membranes with high internal surface area, allowing for a water up-take of up to 99% of the hydrated membrane weight, high

mechanical strength, despite requiring longer culture times and larger cultivation areas **(Campano, Balea, Blanco, & Negro, 2016; Jozala *et al*., 2016)**.

Figure 7 – Hydrated BC membrane grown under static conditions.

The BC production in agitated conditions generates small pellets, suspended fibres, irregular masses or spherical particles instead of membranes. Microscopically, both methods produce similar structures, though, if produced in agitated conditions, BC fibres are curved and entangled, whilst under static conditions fibres are highly extended. This causes BC produced with agitation to have denser structures **(Figueiredo *et al*., 2014)**. The mechanical strength of BC produced under agitated conditions is lower than that of BC obtained with static methods. Additionally, the agitation process in known to induce mutations on the bacteria that reduce the amount of cellulose produced **(Campano *et al.*, 2016; Jozala *et al*., 2016)** and to have an overall lower yield than the static operation **(Jozala *et al*., 2016)**. However, agitated cultures are considered the most suitable cultivation method to achieve BC production at commercial levels, due to the potentiality to develop higher production rates **(Figueiredo *et al*., 2014)**.

The production of BC shows yields of up to 40% (BC production by glucose substrate consumed), which are high efficiencies for a biotechnological process **(Klemm *et al*., 2011)**. If compared with wood cellulose, cellulose produced by bacteria is highly pure, and the purification processes that are still necessary are comparatively simpler, cheaper and environmentally friendlier **(Cacicedo *et al*., 2015)**. However, for engineering purposes, cellulose produced from plants is favoured for mass production, for its cost effectiveness **(Ummartyotin & Manuspiya, 2015)**.

1.5.2. BC properties

As a material, BC shows a unique set of properties, originated from the specific arrangement of cellulose microfibrils. The BC mechanical properties are derived from the crystalline nano- and micro-fibril structure, presenting a tensile strength ranging from 200 to 300 MPa, and a Young's modulus up to 15-35 GPa **(Cacicedo *et al.*, 2015)**, responsible for a high strength-to-weight ratio **(Panaitescu *et al.*, 2015)** and making BC a strong and light material. BC has a thermal stability superior than many thermoplastic polymers, that lose mechanical properties when heated above 100 ºC (*e.g.* during sterilization processes) **(Cacicedo *et al.*, 2015)**, whereas BC decomposition temperature ranges from 340 to 370 ºC **(Figueiredo *et al.*, 2014)**.

Generally BC is characterized by a nano-dimensional fibre network **(Cacicedo *et al.*, 2015; Campano *et al.*, 2016; Panaitescu *et al.*, 2015)**, responsible for a large specific surface area **(Campano *et al.*, 2016; Figueiredo *et al.*, 2014; Jozala *et al.*, 2016)** and a high aspect ratio **(Campano *et al.*, 2016; Figueiredo *et al.*, 2014)**. This network allows for both a good shape retention **(Jozala *et al.*, 2016)** and stress transfer capacity **(Campano *et al.*, 2016)**.

Additionally, BC is biocompatible, biodegradable **(Campano *et al.*, 2016; Figueiredo *et al.*, 2014; Panaitescu *et al.*, 2015)** and non-toxic. The fact that BC is resistant to human degradation *in vivo*, due to the absence of cellulases in the human body, opens a wide field of medical applications, specially cutaneous ones, though it also limits the BC employability inside the human body **(Figueiredo *et al.*, 2014)**.

These set of properties make BC an ideal substrate for the development of composite materials by the establishment of interactions with other polymers and nanoparticles **(Figueiredo *et al.*, 2014)**.

1.5.3. BC modification

BC has the potentiality to be employed in many and diverse areas; in that sense, specific properties may be preferred and, thus, different additives or medium components can be added to the fermentative medium in order to modify or enhance BC structural or physical properties in a specific manner **(Campano *et al.*, 2016)**. This modification strategy is generally described as *in situ* modification, once it occurs simultaneously with the BC

matrix formation. Another strategy to modify BC is classified as *ex situ* modification, that is performed only after the BC formation **(Cacicedo *et al*., 2015)**.

By the *in situ* modification process, compounds are incorporated into the BC matrix as it is synthesized by bacteria, originating new properties by the modification of the intrinsic structure and biophysical properties of BC. These additional molecules usually interact with cellulose chains hydroxyl groups, forming new hydrogen bridges and becoming part of the cellulose fibril network **(Cacicedo *et al*., 2015)**. These molecules are most often hydrophilic, despite the existence of BC modifications with hydrophobic compounds (*e.g*. poly(caprolactone) **(Figueiredo, Silvestre, Neto, & Freire, 2015)**.

Ex situ modifications only take place after the BC matrix is completely formed, and are usually done through the immersion of the BC matrix in a solution with the additional molecules. However, it has the disadvantage of being reversible, meaning that, depending on the nature of the additional molecule-BC interaction and external conditions, the modifications may be reversible, due to leaching **(Cacicedo *et al*., 2015)**.

1.5.4. BC applications

The specific properties and the wide range of modifications that can be performed in BC as a base material allow for its application on the most diverse fields, including food, biomedical, and electronic, among others **(Ullah, Santos, & Khan, 2016)**.

1.5.4.1. Food applications

In the food industry, BC is considered to be a "generally recognized as safe" (GRAS) product **(Ullah *et al*., 2016)**. As a dietary fibre, BC can be used as an agent in thickening pasty condiments, as a stabilizer for ice creams, in gelling and prevent temperature degradation in some foods (*e.g*., cocoa) and sometimes as fat replacement. Another area of the food industry where BC can be used, as native or modified BC, is in food packaging, in which it is used not as an additive but as a protective film over food **(Cacicedo *et al*., 2015; Ullah *et al*., 2016)**.

1.5.4.2. Medical applications

Due to its biocompatibility, high water retention, porous nanostructure, and mechanical strength, BC finds applications as wound dressing, temporary skin substitute, drug delivery systems and implants **(Figueiredo *et al.*, 2014)**. BC has higher complement activation parameters than conventional graft materials, such as poly(ethylene terephthalate) or expanded PTFE, meaning that it is more easily accepted by the body **(Ullah *et al.*, 2016)**. Additionally, vascularization and collagen synthesis is described to occur in the presence of subcutaneous BC implants **(Cacicedo *et al.*, 2015)**. The development of BC composites further widened the scope of BC medical applications **(Ullah *et al.*, 2016)**. However, BC medical application is limited by the fact that mammals are unable to degrade cellulose *in vivo*, a factor that has to be considered regarding applications other than cutaneous ones **(Cacicedo *et al.*, 2015; Ullah *et al.*, 2016)**.

1.5.4.3. Other applications

BC applications that do not fill into the previous categories are, as an all, remarkable for their diversity. As such, BC can also be applied as matrix for enzyme, cells, nanoparticles, drugs or other polymers immobilization **(Cacicedo *et al.*, 2015; Figueiredo *et al.*, 2014; Ullah *et al.*, 2016)**; in cosmetics **(Ullah *et al.*, 2016)**; in electronics, by the functionalization with conductive or metallic compounds **(Cacicedo *et al.*, 2015; Jozala *et al.*, 2016; Klemm *et al.*, 2011; Panaitescu *et al.*, 2015)**; in the paper industry **(Figueiredo *et al.*, 2014; Jozala *et al.*, 2016; Klemm *et al.*, 2011; Panaitescu *et al.*, 2015)** and in energy production **(Cacicedo *et al.*, 2015; Evans, O'Neill, Malyvanh, Lee, & Woodward, 2003; Gadim *et al.*, 2014, 2015; Gao-peng Jiang *et al.*, 2015; Lin, Liang, Chen, & Lai, 2013)**.

1.5.5. BC-based composites

The structure and nature of BC allows for an immense potential as both matrix and reinforcement partner in the formulation of composite materials, simultaneously, BC limitations and/or characteristics (*e.g.*, no antimicrobial and antioxidant activity, lack of optical transparency, conductivity, magnetism or hydrophobicity), especially for purpose oriented applications, further increase the necessity and potential of BC composites. As

such, different BC composites have been devised for applications in medical and pharmaceutical fields, for electronic and conductivity purposes, in separation and purification processes and for high strength cellulose-based materials preparation **(Shah *et al.*, 2013)**.

Generally, BC composites may be classified according with the nature of the compound/material that is associated with cellulose, such as by their inorganic/organic or polymeric/nanodimentional nature, as schematized in Figure 8 **(Shah *et al.*, 2013)**. In the following sections, a summary of purpose directed BC composites is presented.

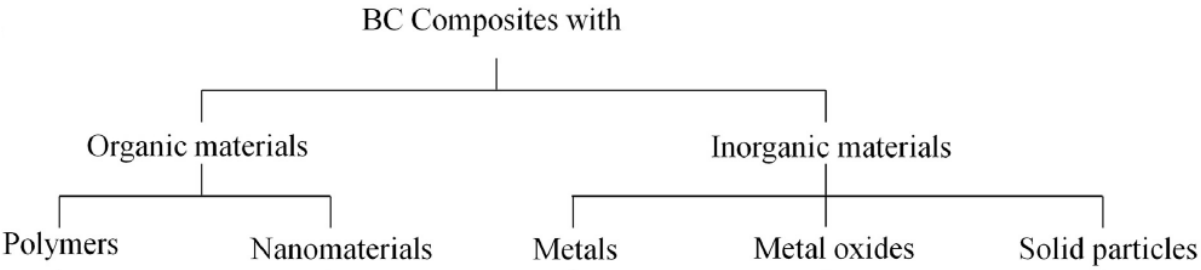

Figure 8 – Classes of materials used in BC-based composites. Adapted from Shah *et al*., 2013.

1.5.5.1. BC-based composites for electronic/conductive purposes

The BC chemical properties and cellulose fiber network allows BC to be used as a matrix for various applications. However, the lack of electric and ionic conductivities, and magnetism, called for the development of composites in order to widen the BC range of application **(Shah *et al.*, 2013)**. In what concerns the need for conductivity and/or magnetism, BC composites have the potentiality to be applied in fuel cells, ion batteries, flexible supercapacitors and other electronic devices **(Xiao Chen *et al.*, 2016)**.

One strategy to produce electron conductive BC matrices is by the formulation of BC composites with metals or with metallic composites, namely nanoparticles, for their general small size and specific behaviour. For this purpose, diverse metals and metallic compounds were combined with BC and studied **(Shah *et al.*, 2013)**.

BC/platinum composites were found to show conductive properties as well as catalytic activities, finding application in fuel cells and as biosensors. Composites of BC with palladium have both conductive and magnetic properties **(Shah *et al.*, 2013)**. BC/gold composites have been utilized as biosensors and other biodevices **(Shah *et al.*, 2013)**. BC/titanium oxide (BC/TiO_2) composites, namely BC/TiO_2 nanofibers are an important

conducting material due to specific electrostatic dipole-dipole interactions established between TiO_2 and cellulose fibres **(Shah *et al.*, 2013)**. BC/iron oxide composites show supermagnetic behaviour at room temperature and can be used in electric and magnetic devices **(Figueiredo *et al.*, 2014; Shah *et al.*, 2013)**.

BC composite materials with conducting polymers are other class of composites with electron conducting properties. The most remarkable polymers that were combined with BC for electron conductivity properties are polyaniline (PANI) and polypyrrole (PPy) **(Xiao Chen *et al.*, 2016; Figueiredo *et al.*, 2014; Shah *et al.*, 2013)**. BC/PANI composites are characterized by the combination of high conductivity and flexibility **(Xiao Chen *et al.*, 2016; Shah *et al.*, 2013)**, and were suggested for application in biosensors, flexible electrodes and flexible displays **(Shah *et al.*, 2013)**. BC/PPy composites are described as having excellent electric conductivity, thermal stability and well-controlled microstructure and were explored as the base for three component composites with $FeCl_3$, ammonium persulphate or carbon nanotubes for enhanced electrical and mechanical properties. Another polymer that has drawn interest for combination with BC is poly(3,4-ethylenedioxythiophene)-poly(styrene-sulfonate) because of its ionic nature and high conductivity **(Xiao Chen *et al.*, 2016)**.

Composites of BC with graphene, graphene oxide and carbon nanotubes were also studied for their electric conductivity properties with promising results for application in carbon/based electronic devices **(Xiao Chen *et al.*, 2016; Shah *et al.*, 2013)**.

The production of ion conductive BC composites is generally performed by the introduction of compounds that enhance and maintain water retention in the BC membrane at high temperatures and low RH. Three chemical groups are described for the production of ion conductive BC membranes, phosphoric acid **(Gaopeng Jiang, Qiao, & Hong, 2012)**, (and phosphoric acid derived compounds **(Vilela, Gadim, Silvestre, Freire, & Figueiredo, 2016)**), phitic acid **(Gaopeng Jiang *et al.*, 2012)** and compounds with sulphonic groups **(Gadim *et al.*, 2014, 2015; Gao-peng Jiang *et al.*, 2015; Lin *et al.*, 2013)**.

Doping BC membranes with solutions of phosphoric acid or phitic acid was one strategy to produce BC composites with proton conductive properties. BC/phosphoric acid membranes show higher proton conductivity than the BC/phitic acid ones. However, the

performance of these composites is lower than that of Nafion® membranes **(Gaopeng Jiang *et al.*, 2012)**.

Another strategy to produce ion conductive BC composites is by the association of BC membranes with polymers carrying sulphonic or phosphoric acid groups. Regarding this strategy, three groups of composites have already been reported: BC/poly(4-styrene sulphonic acid) (PSSA) and BC/poly(2-acrylamido-2-methyl-1-propanesulphonic acid) (PAMPS) **(Gadim *et al.*, 2014; Lin *et al.*, 2013)**; BC/Nafion® composites **(Gadim *et al.*, 2015; Gao-peng Jiang *et al.*, 2015)** and BC/poly(methacryloyloxyethyl phosphate) (PMOEP) **(Vilela *et al.*, 2016)**.

PSSA/BC nanocomposite membranes were prepared by *in situ* free radical polymerization of NaSS inside the BC network. The proton conductivity of this composite is described as being comparable to that of Nafion® membranes **(Gadim *et al.*, 2014)**. This composite will be discussed in further detail in a following section, once it is the focus of the experimental part of this work. BC/PAMPS composites were obtained by UV-grafting of PAMPS onto BC, with proton conductivity results also close to those of Nafion® membranes **(Lin *et al.*, 2013)**.

BC/Nafion® nanocomposites are described as a greener alternative to pure Nafion® membranes, while benefiting from BC intrinsic properties and Nafion® proton conductivity **(Gadim *et al.*, 2015)**. BC/Nafion® composite membranes are generally described as being relatively easy to prepare despite yielding lower performances than pure Nafion® membranes **(Gadim *et al.*, 2015; Gao-peng Jiang *et al.*, 2015)**.

BC/PMOEP nanocomposite membranes were prepared also by the *in situ* polymerization of the monomer methacryloyloxyethyl phosphate (MOEP) in the BC matrix. These membranes are described as having proton conducting properties comparable or even higher than those of Nafion®, as well as maintaining good performances in conditions of high temperatures and low RH **(Vilela *et al.*, 2016)**.

It is worth noting that most these proton conductive BC membranes were suggested for application in fuel cells **(Gadim *et al.*, 2014, 2015; Gao-peng Jiang *et al.*, 2015; Gaopeng Jiang *et al.*, 2012; Lin *et al.*, 2013; Vilela *et al.*, 2016)**.

1.5.6. PSSA/BC nanocomposite membranes

In Gadim *et al*., 2014, a BC nanocomposite with PSSA was developed and characterized. PSSA is an excellent candidate for applications requiring elevated proton conductivity, while simultaneously being a low-cost polymer that is liable to be processed in mild conditions. However, PSSA is a polyelectrolyte, and, therefore, susceptible to dissolution when in a hydrated medium. PSSA was polymerized *in situ*, by free radical polymerization, from NaSS, the monomeric form, to PSSA, to promote a greater polymer integration in the BC matrix. To surpass the natural PSSA susceptibility to dissolution, a bifunctional cross-linking agent, poly (ethylene glycol diacrylate) (PEGDA), was used to enhance the retention of PSSA in the BC membrane matrix. This polymerization reaction is schematized in Figure 9. This work proved that PSSA/BC composites have improved mechanical properties when compared to pure PSSA and protonic conductivities comparable to those of Nafion®.

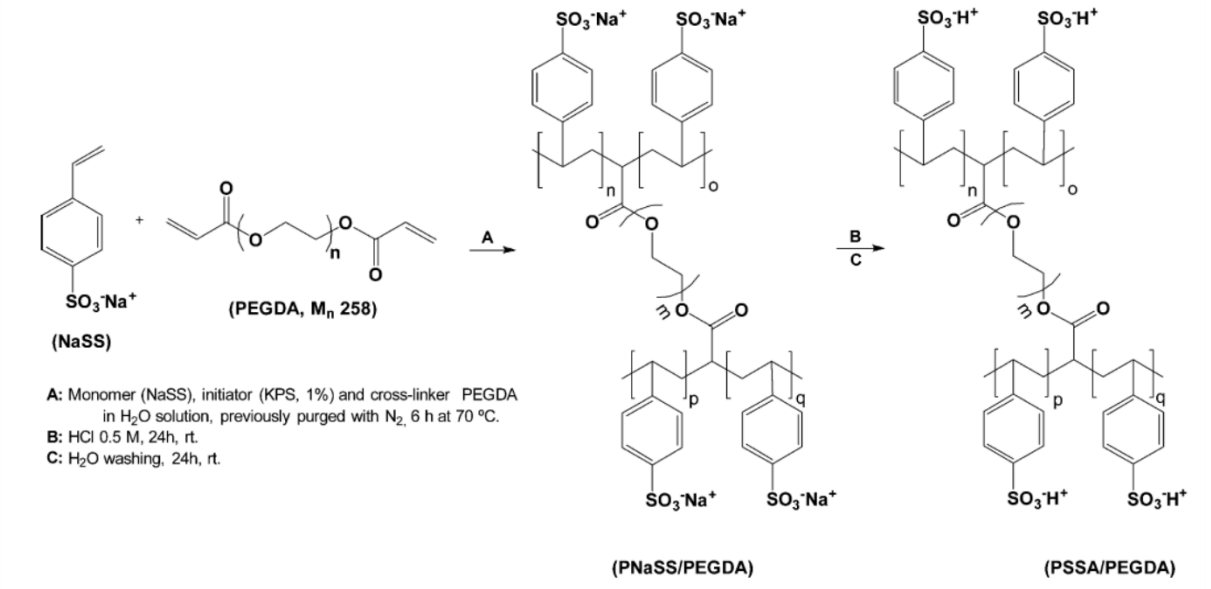

Figure 9 – PSSA polymerization scheme with PEGDA as a cross-linking agent, followed by acidic ionic exchange. Adapted from Gadim *et al.*, 2014.

Afterwards, the same research team further investigated this system, in particular the effects of PSSA/BC anisotropic structure on the membrane protonic conductivity, demonstrating that the proton conductivity is superior on an in-plane membrane configuration, rather than on a through-plane. It was also demonstrated the applicability of

PSSA/BC as a PEM in a fuel cell, with the operation of a PEMFC at room temperature achieving a power density of 40 $mW.cm^{-2}$ **(Gadim *et al*., 2017)**.

1.6. Objectives

In this context, the objective of the present dissertation is to broaden the application spectrum of PSSA/BC composite membranes by studying their applicability as PEM in a single-chamber MFC for electricity production.

2. Experimental section

In this section are described the procedures followed in the preparation of the composite PSSA/BC membranes, as well as the different methods used in for their characterization. This work followed closely the processes and methodologies described by Gadim *et al*., 2014, in which PSSA/BC membranes were prepared with 0, 10, 20 and 40% cross-linking agent and characterized. In this sense, the composite membrane formulation with 10% cross-linking agent was selected for the follow-up work. The obtained nanocomposite membranes were characterized by Fourier transform infrared – attenuated total reflectance spectroscopy (FTIR-ATR), scanning electronic microscopy (SEM), ionic exchange capacity (IEC) and impedance spectroscopy (IS), in order to guarantee the composition and suitability of the obtained PSSA/BC membranes.

After characterization, BC and PSSA/BC membranes were installed on a MFC and the respective operating parameters were registered, namely the polarization and the power density curves.

2.1. Materials and reagents

Sodium-4-vinylbenzene sulfonate (NaSS, 90%), poly(ethylene glycol) diacrylate (PEGDA, M_n 258) and Nafion® 117 were obtained from Sigma-Aldrich, and potassium persulfate (KPS, 98%) was purchased from Panreac. For the HS liquid medium, glucose (96%) was purchased from Sigma-Aldrich and yeast extract and peptone from Himedia. All other chemicals were of analytical grade and used as received.

2.2. BC membrane production

BC membranes were produced by *Gluconacetobacter sacchari* in a HS liquid medium (20 $g.L^{-1}$ glucose, 5 $g.L^{-1}$ peptone, 5 $g.L^{-1}$ yeast extract, 2.7 $g.L^{-1}$ Na_2HPO_4 and 1.15 $g.L^{-1}$ citric acid, pH 5) under static conditions as described by Trovatti *et al*., 2011. After incubation, BC membranes were separated from the media, treated with 0.5 M NaOH to eliminate cells attached to the BC matrix and washed with distilled water to remove culture media components until the registration of neutral pH. Finally, the membranes were whitened with a 1% hypochlorite solution and washed with distilled water. The membranes had a

disk-like shape with approximately 7 cm of diameter and, when hydrated, a thickness of 4-7 mm.

2.3. PSSA/BC composite membrane preparation

PSSA/BC composite membranes were prepared by adaptation of the methodology described by Gadim *et al*., 2014. Hydrated BC membranes were hand pressed several times between two sheets of absorbent paper to drain most of their water content. The membranes dry weight was calculated considering that 99% of their hydrated weight was water. NaSS, KPS (used as polymerization initiator) and PEGDA were weighted and dissolved in a volume of distilled water corresponding to 70% of the water volume drained from the membranes. The reagents weight was determined considering the dry weight of each individual BC membrane. The weight of NaSS corresponded to 5 times the membrane dry weight, that of KPS to 1.2% of the NaSS weight and the weight of PEGDA to 10% of the NaSS weight, following the BC:NaSS:PEGDA relation of 1:5:0.1.

This solution was added to the drained BC membrane, allowing the membrane to absorb the solution for 1 h, in an ice bath and under a N_2 atmosphere. The *in situ* free radical polymerization of NaSS was induced by the heating of the BC membrane to 70 ºC for 6 h, with magnetic agitation.

The obtained PSSA/BC membranes were washed several times and left overnight in distilled water and then dried in an oven for 24 h at 40 ºC. The dried PSSA/BC membranes were converted to the acidic form by ionic exchange with 100 mL of 0.5 M HCl for 24 h and then washed several times with distilled water. The membranes were again dried in an oven for 24 h at 40 ºC and then stored in an exicator for further use.

2.4. PSSA/BC membrane characterization

2.4.1. FTIR-ATR spectroscopy

FTIR-ATR spectra were obtained with a Perkin Elmer Spectrum BX equipment in the 4000 cm^{-1} to 600 cm^{-1}range, with a 4 cm^{-1} resolution and 2 cm^{-1} intervals, after 32 scans and processed with Spectrum™ software.

2.4.2. Scanning electronic microscopy

SEM micrographs of the cross-section and surface of acid-treated PSSA/BC and BC membranes were taken with an HR-FESEM SU-70 Hitachi scanning electronic microscope, operating at 4.0 kV voltage. Surface samples were prepared by gluing membrane fragments to a SEM plate with graphite cement. Cross-section samples were prepared by cracking pieces of the membrane while submerged in liquid N_2 for several minutes. The obtained fragments were slit in graphite cement in order to be attached to the SEM plate, while simultaneously leaving exposed the newly made cross-section. Before the microscopic analysis the membranes were coated with a carbon film.

2.4.3. Ionic exchange capacity (IEC)

The PSSA/BC membranes IEC was determined by titration with a 0.005 M NaOH solution. Approximately one quarter of the membrane was soaked in 25 mL of a 0.1 M NaCl aqueous solution, 24 h prior to the determination. The IEC ($mmol.g^{-1}$) was calculated according with Equation 1:

$$IEC = (V_{NaOH} \times M_{NaOH}).w_d^{-1} \quad \text{Equation 1}$$

where V_{NaOH} is the volume of NaOH (mL) at the equivalence point, M_{NaOH} is the concentration of the NaOH solution (M) and w_d the dry weight of the membrane fragment (g). The IEC determinations were performed in duplicate for each membrane.

2.4.4. Protonic conductivity

Through-plane and in-plane protonic conductivity was determined by impedance spectroscopy (IS) using a Agilent E4980A Precision LCR meter. The samples were painted with silver on both surfaces, in the case of through-plane conductivity and on the extremities of a narrow membrane rectangle, in the case of the in-plane conductivity (Figure 10). The prepared samples were mounted in an electronic apparatus with platinum (Pt) wires and graphite gas diffusion chambers specific for each kind of configuration. The membrane resistance was determined in a climatic chamber (ACS Discovery DY110) where the humidity was set at 30, 60, 80 and 98% RH and the temperatures were varied. Readings were taken at pre-determined temperatures of 40, 60, 80 and 94 ºC. The membrane ohmic resistance corresponds to the extrapolated intersection whit the real axis

of the Nyquist plots obtained with the IS. The membrane protonic conductivity was afterwards calculated according with Equation 2:

$$\sigma = L.(R \times A)^{-1} \qquad \text{Equation 2}$$

where σ is the membrane conductivity ($S.cm^{-1}$), L (cm) corresponds to the membrane thickness, in the case of the through-plane determination and to the distance between the two electrodes on the extremities of the membrane rectangle, in the case of the in-plane determination, R is the measured membrane resistance (Ω) and A is the area (cm^2) of the membrane corresponding to the electrode surface area in the through-plane determination and to the area of the cross-section in the in-plane determination, as illustrated in detail in Figure 10.

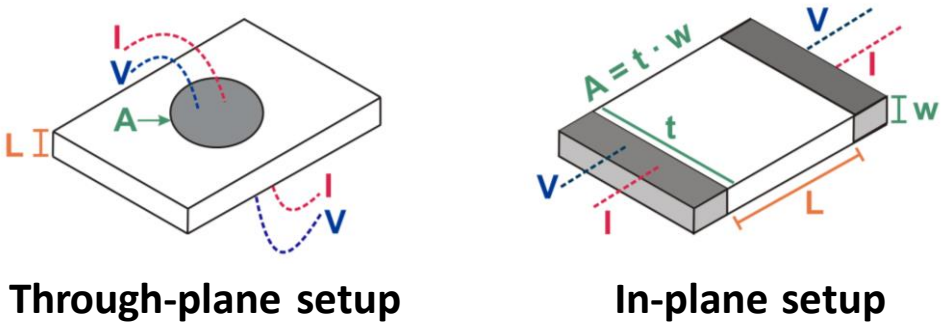

Figure 10 – Schematic representation of the setups of the proton conductivity measured via through-plane and in-plane configuration. Adapted from Gadim *et al.*, 2017.

2.5 Membrane application on microbial fuel cell

BC (in the acidic form), PSSA/BC and Nafion® 117 membranes were assembled in a cylindrical glass MFC (Figure 11a) with a lateral opening of cathode air contact (AnibalFAlves, Portugal), following a single-chamber MFC disposition. A scheme of the MFC assembly is shown in Figure 11b and the respective components description is listed in Table 1.

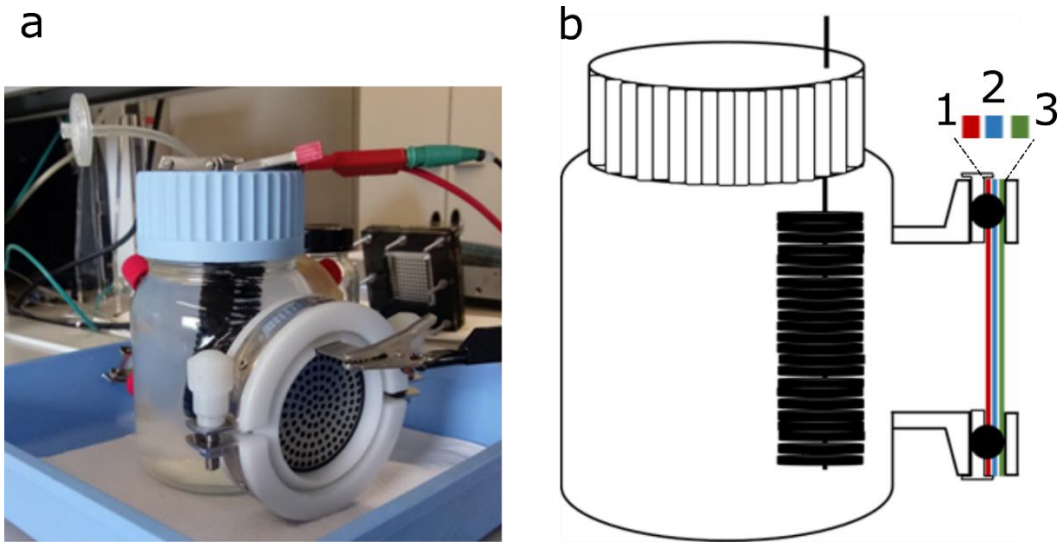

Figure 11 – Assembled MFC, a, and respective schematic representation, b, highlighting the membrane-electrode assembly (MEA): membrane (1), cathode (with diffusion and catalytic layer) (2) and steel collector plaque (3).

Table 1 – Single-chamber MFC components and description.

MFC component	**Description**
Anodic Chamber	900 mL (operational volume).
Anode	Carbon thread brush (Panex 35) and titanium cable: 7.9 cm height and 2.5 cm diameter (Mill-Rose, USA).
Membrane	BC, PSSA/BC or Nafion® 117 membrane.
Cathode	Carbon cloth with a 1.0 $mg.cm^{-2}$ Pt catalytic layer, hydrophobic and microporous layer: 0.27 mm thickness and 5.5 cm diameter (BC-H225-10F, Quintech, Germany).
Current collector	Stainless steel with 143 holes, ø 3 mm (NevesNeves, Portugal).

The MFC anodic chamber was inoculated with *Shewanella frigidimarina* CECT 5932 on a sodium acetate liquid medium (bacterial concentration of 10^7 colony forming units (CFU) mL^{-1}) frequently used on MFC **(Deeke, Sleutels, Hamelers, & Buisman, 2012)**.

The MFC was operated in a sequential fed-batch mode for 7 days (168 h). During this period, the open-circuit voltage (OCV) was measured sporadically, and two polarizations were performed after the stabilization of this parameter. After the first polarization (around 95 h of operation), the cell was replenished with new substrate. For

this, 700 mL of old medium were removed, and an equal volume of sterile medium was added. The MFC was operated at room temperature.

Polarization curves were determined under galvanostatic mode (Zahner Elektrik GmbH & Co. KG), current density intervals of 5 μA were imposed for 3 min and the response voltage (V) was registered. The cell internal resistance was estimated as the slope of the polarization curves in the region of Ohmic losses and expressed in Ω. The MFC resulting power was normalized for the membrane active area and was calculated as power density, $mW.m^{-2}$.

3. Results and Discussion

The present work aimed at studying the applicability of PSSA/BC nanocomposite membranes as PEM in a single-chamber MFC for electricity production. In this perspective, PSSA/BC composite membranes were obtained by the *in situ* free radical polymerization of NaSS in the presence of PEGDA as a cross-linking agent, within the BC network, according to the procedure reported by Gadim *et al.*, 2014. The composite membranes have a predominantly translucent appearance, whereas native BC membranes are opaque, as illustrated in Figure 12.

Figure 12 – Native BC membrane (left) and PSSA/BC nanocomposite membrane (right) both after acidic treatment and dried.

The membranes were characterized in terms of chemical composition (FTIR-ATR spectroscopy), morphology (SEM), ion exchange capacity (IEC) and protonic conductivity. Afterwards the operating parameters of a MFC equipped with BC and PSSA/BC membranes as PEM were determined and compared with the results available in literature.

3.1. PSSA/BC membrane characterization

3.1.1 FTIR-ATR spectroscopy

The FTIR-ATR spectra of BC membrane, PSSA:PEGDA (1:0.1) cross-linked polymer and PSSA/BC nanocomposite membranes (prior to acidic treatment) are shown in Figure 13. The spectrum of the pure BC membrane (Figure 13a) shows the typical absorptions of a cellulosic substrate **(Gadim *et al.*, 2014)**, namely, the absorption band at ~3340 cm^{-1} associated with the hydroxyl groups stretching vibrations (–OH); the absorption at ~2896

cm^{-1} due to the presence of –CH and $–CH_2$ moieties; several absorptions in the 1359-1280 cm^{-1} range associated with –CH and –C–OH groups, this last moiety is also responsible for an absorption at 1107 cm^{-1} and the absorptions in the 1055-1003 cm^{-1} range attributed to the –C–O and –C–O–C– covalent bonds.

On the other hand, the spectrum of the cross-linked PSSA (Figure 13b) shows the band associated with the stretching vibration of –OH groups at ~3340 cm^{-1}, two absorptions at 1179 and 1126 cm^{-1} assigned to the sulfonic groups (SO_3^-), and two more absorptions at 1035 and 1008 cm^{-1} corresponding to the stretching of –C–O and –C–O–C– moieties. The carbonyl (–C=O) absorption at 1720 cm^{-1} **(Gadim *et al.*, 2014)** is not visible in this spectrum, but is supposed to be overlapped with another absorption, as explained ahead.

As expected, the FTIR spectrum of the PSSA/BC membrane (Figure 13c) combines the absorptions of BC and cross-linked PSSA. As such, at ~3340 cm^{-1} is observed the absorption of –OH groups, a feature shared with the both BC and the PSSA; around 2896 cm^{-1} the absorptions of –CH and $–CH_2$ moieties; at 1720 cm^{-1} is present the band of the –C=O absorption; several absorptions in the 1359-1279 cm^{-1} range corresponding to the vibrations of the –C–H and –C–OH bonds; two absorptions at 1179 and 1125 cm^{-1} associated with the SO_3^- group, and, finally, the absorptions in the 1055-1007 cm^{-1} range, attributed to the –C–O and –C–O–C– covalent bonds. Moreover, the success of the *in situ* free radical polymerization of NaSS and the retention of the polymer inside the BC matrix is also confirmed by the presence of the peak at 1599 cm^{-1} associated with PSSA ring skeletal vibration and that at 832 cm^{-1} due to the aromatic out-of-plane C–H deformation (Figure 13c).

A peak at ~1641 cm^{-1} due to the presence of H_2O in the samples **(Gadim *et al.*, 2014)**, is present in all spectra (Figure 13a, b and c). This peak is particularly intense in the PSSA spectrum (Figure 13b) because the PSSA sample, unlike the membranes, was heavily hydrated at the time of the analysis, this H_2O absorption hides the 1720 cm^{-1}, –C=O absorption on the PSSA spectrum.

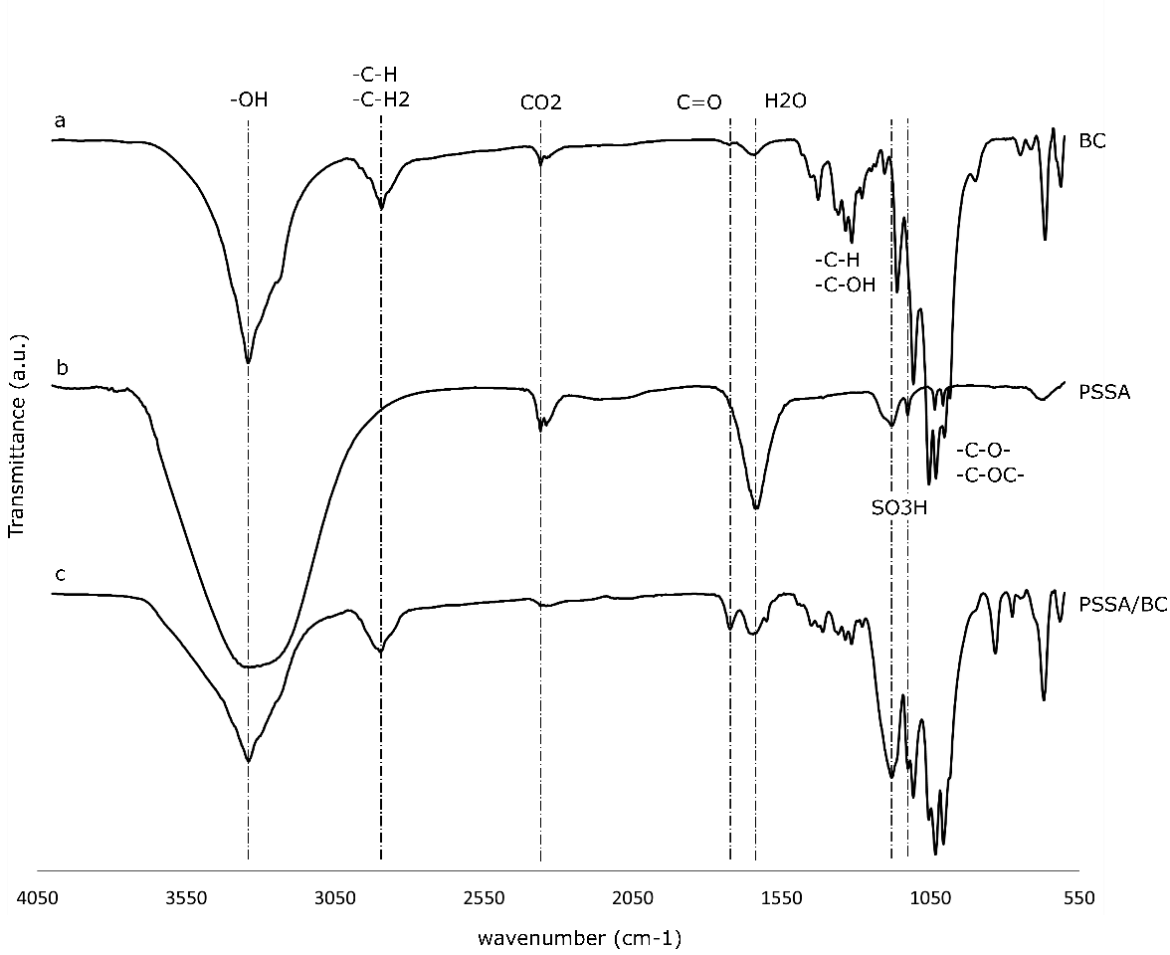

Figure 13- FTIR-ATR spectra of a pure BC membrane, a, hydrated PSSA (PSSA: PEGDA of 1:0.1), b, and a PSSA/BC nanocomposite membrane, c.

As expected, the FTIR spectra of BC membrane before and after acidic treatment are very similar. However, this treatment caused minor alterations on the FTIR-ATR spectrum of the PSSA/BC composite membranes (Appendix Figure A), namely a shift in the profile of the peaks in the range of 1723 to 1599 cm^{-1} from a three-peak outline (Appendix Figure Aa) to a two-peak one (Appendix Figure Ab). This corresponds to the substitution of the sulfonic group coordinated with Na^+ with the protonated sulfonic acid form (SO_3H).

It is also important to emphasize that the uniformity of the distribution and retention of the cross-linked PSSA polymer in the BC matrix was accessed by acquiring FTIR-ATR spectra in different zones of the PSSA/BC membrane, before and after the acidic treatment (Appendix Figure C and Appendix Figure D, respectively).

3.1.2. Scanning electronic microscopy

SEM micrographs of the BC membrane surface (acid treated) are shown in Figure 14 a and c, and those of a PSSA/BC membrane are displayed in Figure 14 b and d. These micrographs show that the *in situ* polymerization only introduces minor changes in the membrane surface morphology, being clear the nanocellulose fibrils network in both BC and PSSA/BC membranes. Notwithstanding, the filling out of the interstices between nanofibrils with PSSA, in the PSSA/BC composite, is confirmed by the protruding nanofibrils, as well as by a higher surface homogeneity (Figure 14d).

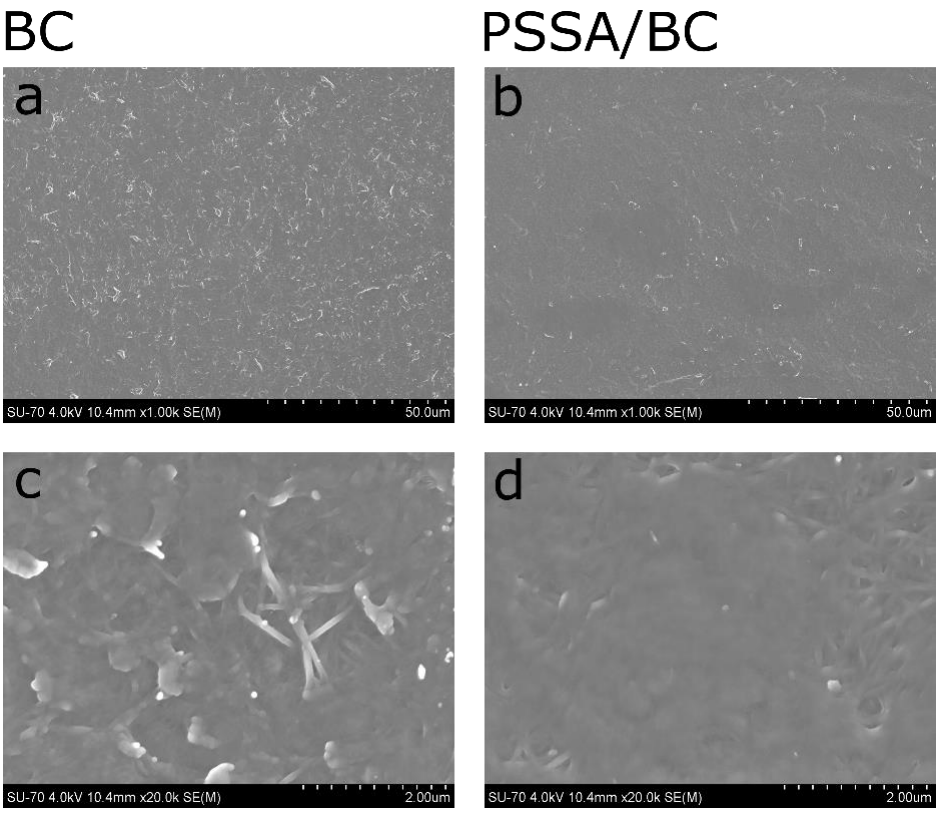

Figure 14 – Surface SEM micrographs of acid treated BC (a and c) and PSSA/BC (b and d) membranes.

SEM micrographs of the cross-section of the acid treated BC and PSSA/BC membranes, are displayed in Figure 15. In these micrographs, it is also possible to observe that the layered morphology as well as the lamellae characteristic structure of BC was only slightly altered by the *in situ* free radical polymerization of NaSS. Particularly, it was perceived a slight thickening of the lamellae after polymerization due to the incorporation

of the cross-linked PSSA in the BC network structure. This incorporation is also responsible for the decrease of the gap width between individual BC lamellae.

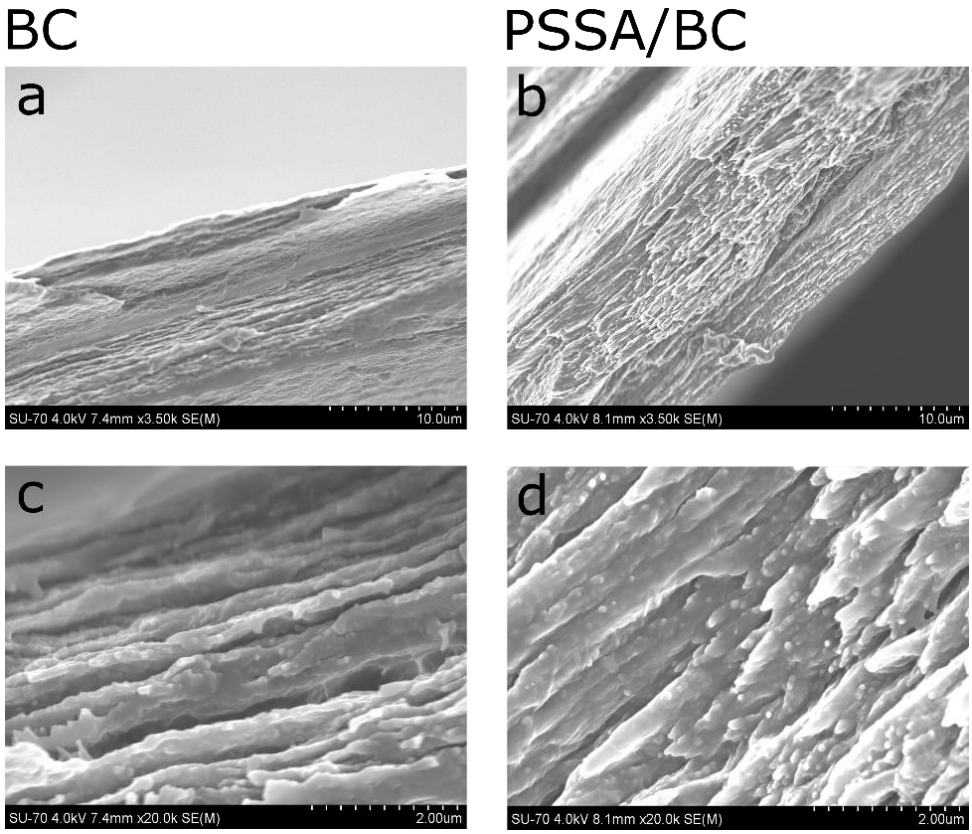

Figure 15 – Cross-section SEM micrographs of acid treated BC, a and c, and PSSA/BC, b and d, membranes.

3.1.3. Ionic exchange capacity

The IEC was calculated as the average of four measures and was found to be equal to 1.85±0.83 mmol.g^{-1}. This value is in agreement with that reported on the literature for PSSA/BC membranes with the same ratio of cross-linking agent (NaSS to PEGDA, 1:0.1), 1.76 mmol.g^{-1} **(Gadim *et al.*, 2014)**. The IEC is related with the amount of H^+ in the PSSA/BC membranes, and therefore with the quantity of sulfonic groups present in the composite; thus, the native BC membranes have a null IEC **(Gadim *et al.*, 2014)**. The IEC value obtained for the PSSA/BC membranes is higher than that of commercially available perflourinated sulfonic acid ionomer membranes, such as Nafion®, that is described as having a minimal IEC of 0.90 mmol.g^{-1} **(Product Bulletin P-12)**. However, the high standard deviation of 0.83 mmol.g^{-1} is an indicator of a significant heterogeneity on the

amount of sulfonic acid moieties and, thus, of PSSA distribution in the distinct PSSA/BC membranes analysed.

3.1.4. Protonic conductivity

The impedance of the PSSA/BC membranes was measured in the through-plane and in-plane configurations as illustrated in Figure 10, which yielded, respectively, the conductivity across the membrane thickness plane and the conductivity along the membrane surface plane. Figure 16 shows the Arrhenius plots for PSSA/BC protonic conductivity under variable conditions of temperature (40, 60, 80 and 94 ºC) and RH (30, 60, 80 and 98%).

The value of 17.3 $mS.cm^{-1}$, at 94 ºC and RH of 98%, is among the highest through-plane conductivity reported for a PSSA/BC membrane with 10% of cross-linking agent (Figure 16a, Table 2). The extreme importance of RH for proton conductivity is evident when comparing the conductivity values, obtained at 80, 60 and 30% RH, and 94ºC, respectively 7.62, 2.11 and 0.125 $mS.cm^{-1}$. Compared with this, the variation of the conductivity in all the other temperature ranges is considerably smaller, highlighting the greater influence of RH rather than temperature on the proton conduction processes.

The in-plane protonic conductivity (Figure 16b) is remarkably higher than that measured on a through-plane configuration (Figure 16a), reaching a maximum of 344 $mS.cm^{-1}$ for 80 ºC at 98% RH. In this configuration, the RH remains highly significant, with the values, for 80 ºC, decreasing from 72.8 to 0.892 $mS.cm^{-1}$ in the range of RH of 80 to 30%. Contrary to what is expected, the in-plane conductivity values were lower at 94 ºC than at 80 ºC, within the whole RH range. This shift resembles a change of membrane behaviour from Arrhenius to Vogel-Tamman-Fulcher (VTF) model, which is associated with alterations on the proton transport mechanisms from a predominantly structural diffusion to a transport based on the segmental motions of cross-linked PSSA. However, this shift is reported to happen at lower RH **(Gadim *et al.*, 2017)** and not at high temperatures.

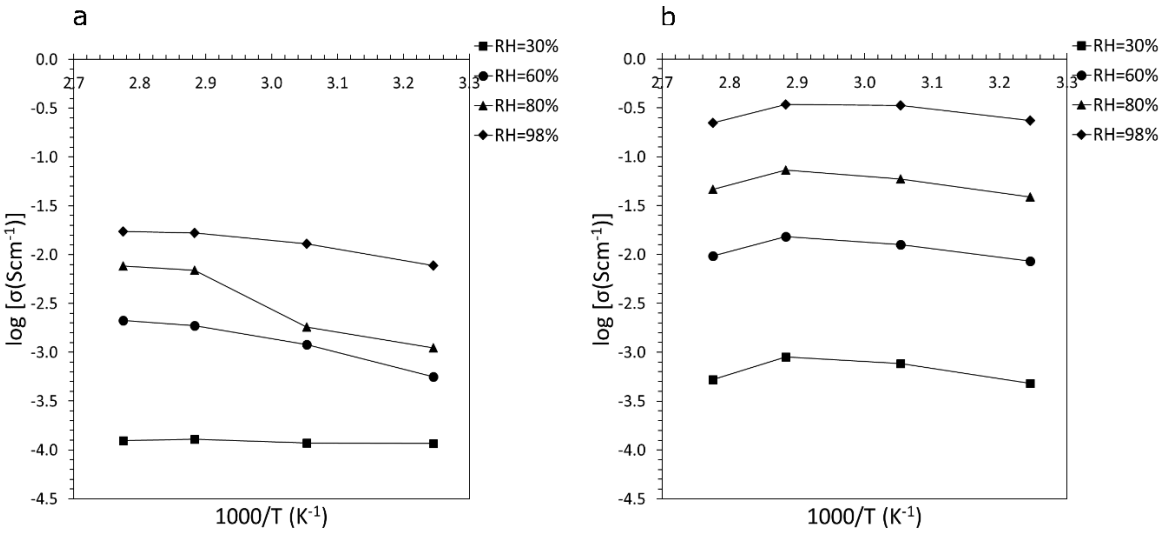

Figure 16 – Protonic conductivity of selected PSSA/BC membrane measured in through-plane, a, and in-plane disposition, b.

The natural anisotropic behaviour of the BC membrane is responsible for the different protonic conductivities registered on the same PSSA/BC membrane sample and for the same conditions of temperature and RH, but at different configurations. In this way, the conductivities in the in-plane configuration are consistently superior than those of the through-plane. This behaviour is induced by the typical BC lamellar morphology as shown by the SEM images in Figure 15c and d. The PSSA polymerization along the BC lamellae (which align with the plane of the membrane) originates a more continuous phase along this plane, that is more favourable to the proton conduction than the more heterogeneous through-plane phase **(Gadim *et al.*, 2017)**. Once again, with increasing RH, the effect of water as a plasticizer of the PSSA structure, allows a higher mobility and a more pseudo-homogenous phase, leading to higher proton conductivities up to the point where proton structural diffusion between water layers becomes the predominant mechanism for proton transport **(Gadim *et al.*, 2014)** and the influence of the anisotropic behaviour is reduced. It was described that for maximum temperature and RH conditions (94 ºC, 98% RH), the conductivity values of both configurations converge **(Gadim *et al.*, 2017)**, though this tendency was not observed in this work (Figure 16a and b). This is indicative that at least the membrane on the through-plane configuration, or both, were unable to achieve a level of saturated hydration at which the structural diffusion of protons should be able to surpass the constraints in conduction induced by the through-plane configuration.

Comparing the PSSA/BC protonic conductivity with that of acid treated BC (Figure 17) is clear the influence of the polyelectrolyte nature of PSSA (presence of sulfonic acid groups on the PSSA structure) on the overall PSSA/BC membrane conductivity. As reference, the BC best conductivity values, measured at 94 ºC and 98% RH (0.00158 $mS.cm^{-1}$) are still much lower than those of the through-plane conductivity of PSSA/BC at 30% RH and 94 ºC (0.125 $mS.cm^{-1}$).

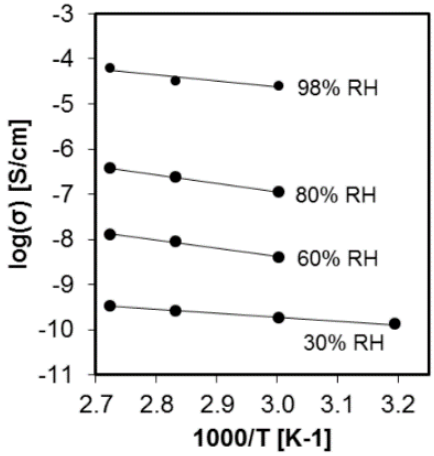

Figure 17 – Through-plane protonic conductivity of acid treated BC. Adapted from the supporting information of Gadim *et al*., 2014.

In table 2 and 3 are shown some protonic conductivity values for PSSA/BC and Nafion® membranes, found in the literature, in the in-plane and through-plane configurations, respectively. To note that although some of those results were determined at different temperatures, they were all obtained in conditions of saturated RH.

The direct comparison with the works of Gadim *et al*., 2014 and Gadim *et al*., 2017 allows to determine that the PSSA/BC membranes prepared in this work have a through-plane proton conductivity that sits between the values of those two works. Notwithstanding, these membranes and those of Gadim *et al*., 2014 follow the same formulation, with 10% of cross-linking agent PEGDA, whereas those of Gadim *et al*., 2017 have a higher content (20 or 40%) of cross-linking agent (Table 2).

The obtained through-plane proton conductivity is, as such, in accordance with what is considered a good value for a PEM to be installed in a PEMFC, 10 $mS.cm^{-1}$, **(Bakangura *et al*., 2015)**. Despite the inexistence of a consensus regarding the protonic conductivity of Nafion® **(Gadim *et al*., 2017; Product Bulletin P-12; Pereira *et al*., 2008),** which derives from the existence of different specifications for this material, the

commercial value of 100 $mS.cm^{-1}$ is advanced, which is considerably higher that obtained in this work. The fact that Nafion® is described as having a higher protonic conductivity than the PSSA/BC membrane, even though it has a lower IEC, can only be supposed to be associated with an overall higher efficiency in proton transport that is independent from the amount of sulfonic groups present in the membranes.

Table 2- Membrane through-plane protonic conductivity. The percentages indicated near the PSSA/BC membranes correspond to the content of PEGDA used in each membrane.

Membranes	**Conductivity ($S.cm^{-1}$)**	**T (ºC)**	**RH (%)**	**Reference**
PSSA/BC (10%)	0.0173	94	98	this work
PSSA/BC (10%)	0.004	94	98	Gadim *et al*., 2014
PSSA/BC (40%)	0.088	26	98	Gadim *et al*., 2017
PSSA/BC (20%)	0.0054	26	98	Gadim *et al*., 2017
Nafion®	0.10	25	100	Product Bulletin P-12.

Table 3 – Membrane in-plane protonic conductivity.

Membranes	**Conductivity ($S.cm^{-1}$)**	**T (ºC)**	**RH (%)**	**Reference**
PSSA/BC (10%)	0.344	80	98	this work
Nafion®	0.08	80	100	Clochard *et al*., 2010

3.2. PSSA/BC membrane application on microbial fuel cell

After the characterization of the PSSA/BC nanocomposite in terms of structure, morphology and protonic conductivity, the membrane was tested as a separator in a single-chamber MFC for energy production. For comparison purposes, membranes of pure BC (after acidic treatment) and Nafion® 117 were also tested under the same conditions. Furthermore, two polarization and power density curves were obtained for each membrane, namely after 95 and 167 h of MFC operation.

Figure 18 shows the first and second polarization (a and b) and power density (c and d) curves of the BC membrane. It is immediately visible from these curves that the

open-circuit voltage (OCV) of BC increased from 0.352 V after 95 h to 0.427 V after 167 h. A similar increase in performance is observed for the power density, in which the MFC operating with the BC membrane yields a maximum power density of 1.46 $mW.m^{-2}$ at a current density of 6.31 $mA.m^{-2}$ after 95 h, and of 2.30 $mW.m^{-2}$ at a current density of 8.42 $mA.m^{-2}$ after 167 h. The internal resistance obtained for both polarization curves was determined as 1.48×10^4 Ω for the first and as 1.44×10^4 Ω for the second polarizations. The results of the OCV and power density are perfectly suited with the expected for a MFC operating under a fed-batch regime, considering that the second polarization was performed after the replenishment of the cell with new substrate, in a moment where the bacteria were already adapted to the cell conditions, and were able to reach higher metabolic thresholds, thus yielding higher power densities.

In Ko, Oh, & Lee, 2015, a MFC was operated with BC as PEM, yielding a maximum power density of 195 $mW.m^{-2}$, a value that is nearly 100 times higher than that obtained in this work. However, several differences in cell architecture and operation between these two works must be noted. First, the MFC used by these authors was a double-chamber MFC with an operational volume of up to 24 L with an environmental mixed bacterial consortium and an artificial electron mediator (Neutral Red) that was employed to facilitate the electron transfer from the bacteria to the anode. Secondly, and most importantly, their BC membrane was chemically modified to have carboxylic groups, which increased the membrane proton conductivity **(Ko *et al*., 2015)**.

The MFC operation with a Nafion® 117 PEM had a OCV of 0.334 V and 0.430 V on the first (95 h) and second (167 h) polarizations, respectively. The maximum power density followed a similar trend, with 0.61 $mW.m^{-2}$ at a current density of 4.21 $mA.m^{-2}$ and 1.55 $mW.m^{-2}$ at a current density of 6.31 $mA.m^{-2}$ (Figure 18c and d). However, the internal resistance, decreased from 2.24×10^4 to 1.51×10^4 Ω. The OCV and power density results are surprisingly low for a Nafion® membrane applied to a MFC. Considering the power density as a reference parameter for MFC performance, the registered maximum power density of 1.55 $mW.m^{-2}$ is remarkably low. Although the high variability of Nafion® equipped MFC power densities found in the literature (*e.g.*, 8.09 $mW.m^{-2}$ **(Vilas Boas *et al*., 2015)**; 30.2 $mW.m^{-2}$ **(Lóránt, Lóka, & Tardy, 2015)**; 262 $mW.m^{-2}$ **(Liu Hong, 2004)**) and considering the many differences in MFC setup and operation, these results show that the MFC operated in this work may be prone to low performances.

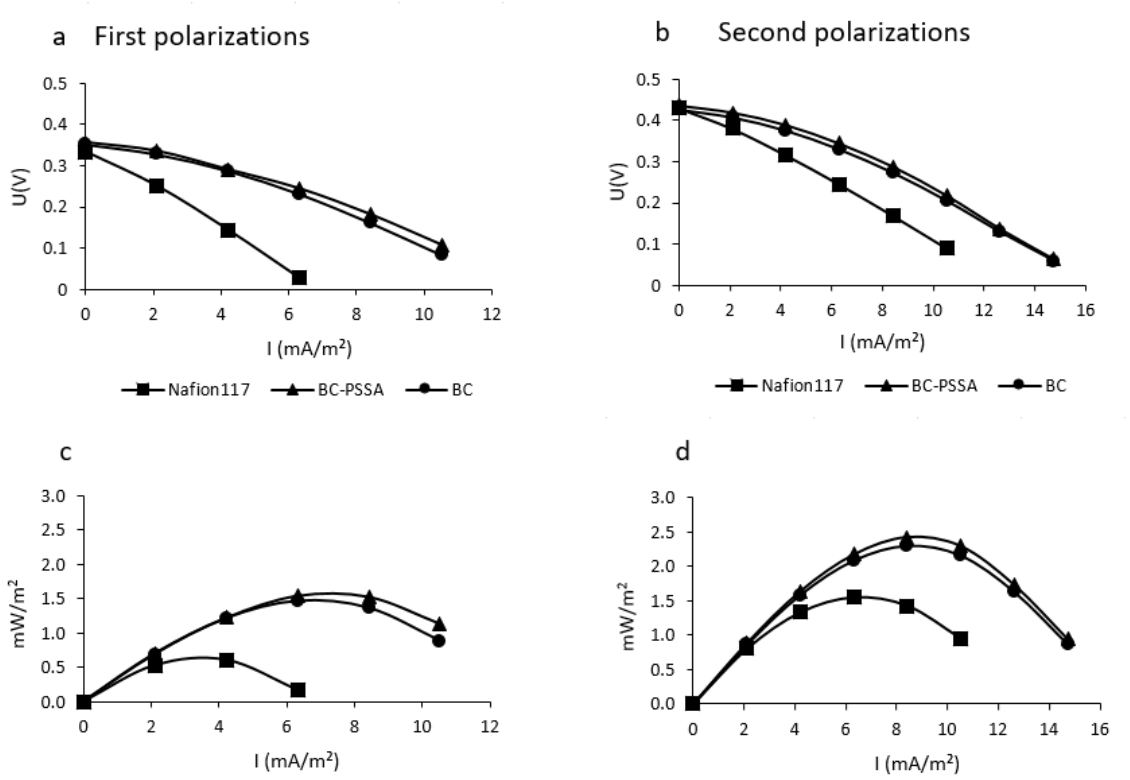

Figure 18 – First (a) and second (b) polarization curves, and first (c) and second (d) power density curves for membranes of BC, Nafion® and PSSA/BC.

Regarding the MFC operation with the PSSA/BC nanocomposite membrane (Figure 18), the OCV was determined to be of 0.357 V and 0.436 V, with a maximum power density of 1.55 $mW.m^{-2}$, at a current density of 6.31 $mA.m^{-2}$, and of 2.42 $mW.m^{-2}$, at a current density of 8.42 $mA.m^{-2}$, and an internal resistance of 1.37×10^{4} Ω and 1.51×10^{4} Ω, on the first and second polarizations, respectively. Yet again, the general tendency for a higher performance on the second polarization and after the partial substitution of the culture medium was observed.

To our knowledge, there is no description on the literature about the application of PSSA/BC membranes on a MFC. The closest reference is supplied by Gadim *et al*., 2017, that operated an air-hydrogen PEMFC equipped with a PSSA/BC membrane that yielded a power density of 400 $W.m^{-2}$. In this sense, the power density of 2.42 $mW.m^{-2}$ is much lower, though completely justified considering the inherent differences of these two systems.

On the second polarisation, the PSSA/BC membrane achieved a maximum power density of 2.42 $mW.m^{-2}$ and Nafion® of 1.55 $mW.m^{-2}$. These values were not expected,

once Nafion® is often considered the reference PEM for laboratorial, commercial, MFC or air-hydrogen applications alike **(Leong *et al.*, 2013)**. In these sense, further studies will be required to fully understand the reason behind the higher performance of the MFC operating with a PSSA/BC membrane than with Nafion®.

Additionally, the results of the MFC operation with BC (acid treated) and PSSA/BC membranes yielded unexpectedly similar results. On the second polarizations, the OCV and the internal resistance values are strikingly close, and the maximum power density of the PSSA/BC membrane is only 0.12 $mW.m^{-2}$ higher than that of BC (Figure 18 d). An explanation for this, as already hinted by the Nafion® membrane low performance, is the fact that the BC and PSSA/BC membranes have already achieved the highest MFC operating threshold, operating with this setup and under these conditions. This fact suggests that other factors, such as slow bacterial metabolism, low bacterial electron transfer rate to the electrode or the kinetics of O_2 reduction on the cathode may be limiting the MFC performance **(ElMekawy *et al.*, 2013)**. Which is further illustrated by comparing the results obtained for the resistance of the PSSA/BC membranes (used to calculate the protonic conductivity) and those of the MFC internal resistance. Indeed, when the composite membrane has resistances around 1 Ω, the cell has internal resistances up to 4 orders of magnitude higher.

4. Conclusions

PSSA/BC nanocomposite membranes were effectively prepared by *in situ* free radical polymerization of NaSS within the swollen BC three-dimensional network under green reaction conditions. The nanocomposite membranes show an IEC of 1.85 ± 0.83 $mmol.g^{-1}$, and anisotropic proton conductance with an in-plane conductivity (344 $mS.cm^{-1}$, 80 ºC at 98% RH) higher than that of the through-plane (17.3 $mS.cm^{-1}$, 94 ºC at 98% RH) due to the anisotropic morphology found in the membranes.

The MFC operation with a BC membrane yielded what was considered a low performance in terms of internal resistance and power density. The former was high (1.44×10^4 Ω) whereas the latter was low (maximum of 2.30 $mW.m^{-2}$). When applied to a MFC, the PSSA/BC obtained similar results, with a power density of 2.42 $mW.m^{-2}$ and an internal resistance of 1.51×10^4 Ω. The power density results were, however, superior than those obtained with Nafion®, which is generally recognized as the reference PEM. This fact together with the similar results with native and composite membranes, allows to conclude that the MFC performance is much likely limited by other factors.

Among the possible lines of future work to continue this study, it would be interesting to tackle the following topics:

- To understand the reason why the MFC operating with a PSSA/BC membrane, as proton exchange membrane, was superior in performance when compared with Nafion®;
- To determine the wastewater treatment potentiality of a MFC with PSSA/BC membranes, with simultaneous energy production, focusing on the optimization of both processes;
- To perform a comparative study to assess the possibility of using BC-based proton exchange membranes containing different protogenic groups as separators in MFCs for both energy production and wastewater treatment.

5. References

Bakangura, E., Wu, L., Ge, L., Yang, Z., & Xu, T. (2015). Mixed matrix proton exchange membranes for fuel cells: state of the art and perspectives. *Progress in Polymer Science*, *57*, 103–152. http://doi.org/10.1016/j.progpolymsci.2015.11.004

Buch-Pedersen, M. J., Pedersen, B. P., Veierskov, B., Nissen, P., & Palmgren, M. G. (2009). Protons and how they are transported by proton pumps. *Pflugers Archiv European Journal of Physiology*, *457*(3), 573–579. http://doi.org/10.1007/s00424-008-0503-8

Cacicedo, M. L., Castro, M. C., Servetas, I., Bosnea, L., Boura, K., Tsafrakidou, P., Castro, G. R. (2015). Progress in bacterial cellulose matrices for biotechnological applications. *Bioresource Technology*, *213*, 172–180. http://doi.org/10.1016/j.biortech.2016.02.071

Campano, C., Balea, A., Blanco, A., & Negro, C. (2016). Enhancement of the fermentation process and properties of bacterial cellulose: a review. *Cellulose*, *23*(1), 57–91. http://doi.org/10.1007/s10570-015-0802-0

Chen, X., Wang, Y., Zhao, Y., & Zhou, Y. (2016). A study of double functions and load matching of a phosphoric acid fuel cell/heat-driven refrigerator hybrid system. *Energy*, *101*, 359–365. http://doi.org/10.1016/j.energy.2016.02.029

Chen, X., Yuan, F., Zhang, H., Huang, Y., Yang, J., & Sun, D. (2016). Recent approaches and future prospects of bacterial cellulose-based electroconductive materials. *Journal of Materials Science*, *51*(12), 1–16. http://doi.org/10.1007/s10853-016-9899-2

Clochard, M., Berthelot, T., Baudin, C., Betz, N., Balanzat, E., Gébel, G., & Morin, A. (2010). Ion track grafting : A way of producing low-cost and highly proton conductive membranes for fuel cell applications. *Jornal of Power Sources*, *195*, 223–231. http://doi.org/10.1016/j.jpowsour.2009.07.016

Deeke, A., Sleutels, T. H. J. A., Hamelers, H. V. M., & Buisman, C. J. N. (2012). Capacitive Bioanodes Enable Renewable Energy Storage in Microbial Fuel Cells. *Environmental and Science Technology*, 46, 3552–3560. http://doi.org/10.1021/es204126r

Di, V., Piga, M., Giffin, G. A., & Pace, G. (2012). Broadband electric spectroscopy of proton conducting SPEEK membranes. *Jornal of Power Sources*, *391*, 58–67. http://doi.org/10.1016/j.memsci.2011.10.049

Du, Z., Li, H., & Gu, T. (2007). A state of the art review on microbial fuel cells: A promising technology for wastewater treatment and bioenergy. *Biotechnology Advances*, *25*(5), 464–482. http://doi.org/10.1016/j.biotechadv.2007.05.004

Dutta, K., & Kundu, P. P. (2014). A Review on Aromatic Conducting Polymers-Based Catalyst Supporting Matrices for Application in Microbial Fuel Cells. *Polymer Reviews*, *54*(3), 401–435. http://doi.org/10.1080/15583724.2014.881372

Eichhorn, S. J., Dufresne, A., Aranguren, M., Marcovich, N. E., Capadona, J. R., Rowan, S. J., Peijs, T. (2010). Review: Current international research into cellulose nanofibres and nanocomposites. *Journal of Materials Science* ,Vol. 45, 1–33. http://doi.org/10.1007/s10853-009-3874-0

ElMekawy, A., Hegab, H. M., Dominguez-Benetton, X., & Pant, D. (2013). Internal resistance of microfluidic microbial fuel cell: Challenges and potential opportunities. *Bioresource Technology*, *142*, 672–682. http://doi.org/10.1016/j.biortech.2013.05.061

Evans, B. R., O'Neill, H. M., Malyvanh, V. P., Lee, I., & Woodward, J. (2003). Palladium-bacterial cellulose membranes for fuel cells. *Biosensors and Bioelectronics*, *18*(7), 917–923. http://doi.org/10.1016/S0956-5663(02)00212-9

Ferreira Mercuri, E. G., Jakubiak Kumata, A. Y., Amaral, E. B., & Simões Vitule, J. R. (2016). Energy by Microbial Fuel Cells: Scientometric global synthesis and challenges. *Renewable and Sustainable Energy Reviews*, *65*, 832–840. http://doi.org/10.1016/j.rser.2016.06.050

Figueiredo, A. R. P., Silvestre, A. J. D., Neto, C. P., & Freire, C. S. R. (2015). In situ synthesis of bacterial cellulose / polycaprolactone blends for hot pressing nanocomposite films production. *Carbohydrate Polymers*, *132*, 400–408. http://doi.org/10.1016/j.carbpol.2015.06.001

Figueiredo, A. R. P., Vilela, C., Neto, C. P., Silvestre, A. J. D., & Freire, C. S. R. (2014). Bacterial Cellulose-Based Nanocomposites: Roadmap for Innovative Materials. *Nanocellulose Polymer Nanocomposites: Fundamentals and Applications*, 17–64. http://doi.org/10.1002/9781118872246.ch2

Gadim, T. D. O., Figueiredo, A. G. P. R., Rosero-navarro, N. C., Vilela, C., Gamelas, J. A. F., Barros-timmons, A., Figueiredo, F. M. L. (2014). Nanostructured Bacterial Cellulose − Poly(4-styrene sulfonic acid) Composite Membranes with High Storage Modulus and Protonic Conductivity. *Applied Materials and Interfaces*, *6*, 7864–7875. http://doi.org/dx.doi.org/10.1021/am501191t |

Gadim, T. D. O., Loureiro, F. J. A., Vilela, C., Rosero-navarro, N., Silvestre, A. J. D., Freire, C. S. R., & Figueiredo, F. M. L. (2017). Electrochimica Acta Protonic conductivity and fuel cell tests of nanocomposite membranes based on bacterial cellulose. *Electrochimica Acta*, *233*, 52–61. http://doi.org/10.1016/j.electacta.2017.02.145

Gadim, T. D. O., Vilela, C., Loureiro, F. J. A., Silvestre, A. J. D., Freire, C. S. R., & Figueiredo, F. M. L. (2015). Nafion® and nanocellulose: A partnership for greener polymer electrolyte membranes. *Industrial Crops and Products*, *93*, 212–218. http://doi.org/10.1016/j.indcrop.2016.01.028

Giffin, G. A., Piga, M., Lavina, S., Assunta, M., Epifanio, A. D., Scrosati, B., & Di, V. (2012). Characterization of sulfated-zirconia / Nafion ® composite membranes for proton exchange membrane fuel cells. *Jornal of Power Sources*, *198*, 66–75. http://doi.org/10.1016/j.jpowsour.2011.09.093

Habibul, N., Hu, Y., & Sheng, G.-P. (2016). Microbial fuel cell driving electrokinetic remediation of toxic metal contaminated soils. *Journal of Hazardous Materials*, *318*, 9–14. http://doi.org/10.1016/j.jhazmat.2016.06.041

Haile, S. M. (2003). Fuel cell materials and components. *Acta Materialia*, *51*(19), 5981–6000. http://doi.org/10.1016/j.actamat.2003.08.004

Hickner, M. A., Ghassemi, H., Kim, Y. S., Einsla, B. R., Mcgrath, J. E., Hickner, M. A., Mcgrath, J. E. (2004). Alternative Polymer Systems for Proton Exchange Membranes (PEMs) Alternative Polymer Systems for Proton Exchange Membranes (PEMs). *Chemical Reviews 104*(10), 4587–4612. http://doi.org/10.1021/cr020711a

Jiang, G., Qiao, J., & Hong, F. (2012). Application of phosphoric acid and phytic acid-doped bacterial cellulose as novel proton-conducting membranes to PEMFC. *International Journal of Hydrogen Energy*, *37*(11), 9182–9192. http://doi.org/10.1016/j.ijhydene.2012.02.195

Jiang, G., Zhang, J., Qiao, J., Jiang, Y., Zarrin, H., Chen, Z., & Hong, F. (2015). Bacterial nanocellulose/Nafion composite membranes for low temperature polymer electrolyte fuel cells. *Journal of Power Sources*, *273*, 697–706. http://doi.org/10.1016/j.jpowsour.2014.09.145

Jozala, A. F., de Lencastre-Novaes, L. C., Lopes, A. M., de Carvalho Santos-Ebinuma, V., Mazzola, P. G., Pessoa-Jr, A., Chaud, M. V. (2016). Bacterial nanocellulose production and application: a 10-year overview. *Applied Microbiology and Biotechnology*, *100*(5), 2063–2072. http://doi.org/10.1007/s00253-015-7243-4

Kamarudin, S. K., Achmad, F., & Daud, W. R. W. (2009). Overview on the application of direct methanol fuel cell (DMFC) for portable electronic devices. *International Journal of Hydrogen Energy*, *34*(16), 6902–6916. http://doi.org/10.1016/j.ijhydene.2009.06.013

Kim, D. J., Jo, M. J., & Nam, S. Y. (2015). Journal of Industrial and Engineering Chemistry A review of polymer – nanocomposite electrolyte membranes for fuel cell application. *Journal of Industrial and Engineering Chemistry*, *21*, 36–52. http://doi.org/10.1016/j.jiec.2014.04.030

Klemm, D., Kramer, F., Moritz, S., Lindström, T., Ankerfors, M., Gray, D., & Dorris, A. (2011). Nanocelluloses: A new family of nature-based materials. *Angewandte Chemie - International Edition*, *50*(24), 5438–5466. http://doi.org/10.1002/anie.201001273

Ko, Y. H., Oh, H. J., & Lee, H. J. (2015). Microbial & Biochemical Technology Use of Bacterial Cellulose from Gluconacetobacter hansenii NOK21 as a Proton-permeable Membrane in Microbial Fuel Cells. *Jornal of Microbial and Biochemical Technology 7*(3), 145–151.

http://doi.org/10.4172/1948-5948.1000196
Larminie, J., & Dicks, A. (2001). *Fuel Cell Systems Explained*. *Journal of Power Sources* (Vol. 93). http://doi.org/10.1016/S0378-7753(00)00571-1
Leong, J. X., Daud, W. R. W., Ghasemi, M., Liew, K. Ben, & Ismail, M. (2013). Ion exchange membranes as separators in microbial fuel cells for bioenergy conversion: A comprehensive review. *Renewable and Sustainable Energy Reviews*, *28*, 575–587. http://doi.org/10.1016/j.rser.2013.08.052
Lin, C. W., Liang, S. S., Chen, S. W., & Lai, J. T. (2013). Sorption and transport properties of 2-acrylamido-2-methyl-1-propanesulfonic acid-grafted bacterial cellulose membranes for fuel cell application. *Journal of Power Sources*, *232*, 297–305. http://doi.org/10.1016/j.jpowsour.2013.01.047
Liu Hong, L. E. B. (2004). Electricity Generation Using an Air-Cathode Single Chamber Microbial Fuel Cell in the Presence and Absence of a Proton Exchange Membrane. *Environmental Science and. Technology.* , *38*,(14), 4040–4046. http://doi.org/10.1021/es0499344
Logan, B. E. (2009). Exoelectrogenic bacteria that power microbial fuel cells. *Nature Reviews Microbiology*, *7*, 375–381. http://doi.org/10.1038/nrmicro2113
Logan, B. E., Hamelers, B., Rozendal, R., Schröder, U., Keller, J., Freguia, S., Rabaey, K. (2006). Microbial fuel cells: Methodology and technology. *Environmental Science and Technology*, *40*(17), 5181–5192. http://doi.org/10.1021/es0605016
Logan, B. E., & Regan, J. M. (2006). Electricity-producing bacterial communities in microbial fuel cells. *Trends in Microbiology*, *14*(12), 512–518. http://doi.org/10.1016/j.tim.2006.10.003
Lóránt, B., Lóka, M., & Tardy, G. M. (2015). Substrate Concentration Dependency of Electricity Production in Microbial Fuel Cells, 1–7.
Mehmeti, A., McPhail, S. J., Pumiglia, D., & Carlini, M. (2016). Life cycle sustainability of solid oxide fuel cells: From methodological aspects to system implications. *Journal of Power Sources*, *325*, 772–785. http://doi.org/10.1016/j.jpowsour.2016.06.078
E.I. du Pont de Nemours and Company, DuPont Fuel Cells, DuPont Nafion PFSA Membranes N115, N117, N1110. Product Bulletin P-12, 1-3.
Milner, E. M., Popescu, D., Curtis, T., Head, I. M., Scott, K., & Yu, E. H. (2016). Microbial fuel cells with highly active aerobic biocathodes. *Journal of Power Sources*, *324*, 8–16. http://doi.org/10.1016/j.jpowsour.2016.05.055
Minh, N. Q. (2004). Solid oxide fuel cell technology — features and applications. *Solid State Ionics*, *174*, 271–277. http://doi.org/10.1016/j.ssi.2004.07.042
Moon, R. J., Martini, A., Nairn, J., Simonsen, J., & Youngblood, J. (2011). Cellulose nanomaterials review: structure, properties and nanocomposites. *Chemical Society Reviews* (Vol. 40). http://doi.org/10.1039/c0cs00108b
Nechyporchuk, O., Belgacem, M. N., & Bras, J. (2015). Production of cellulose nanofibrils: A review of recent advances. *Industrial Crops and Products*, *93*, 2–25. http://doi.org/10.1016/j.indcrop.2016.02.016
Oliveira, V. B., Simões, M., Melo, L. F., & Pinto, A. M. F. R. (2013). Overview on the developments of microbial fuel cells. *Biochemical Engineering Journal*, *73*, 53–64. http://doi.org/10.1016/j.bej.2013.01.012
Pachauri, R. K., & Chauhan, Y. K. (2015). A study, analysis and power management schemes for fuel cells. *Renewable and Sustainable Energy Reviews*, *43*, 1301–1319. http://doi.org/10.1016/j.rser.2014.11.098
Panaitescu, D. M., Frone, A. N., & Chiulan, I. (2015). Nanostructured biocomposites from aliphatic polyesters and bacterial cellulose. *Industrial Crops and Products*, *93*, 251–266. http://doi.org/10.1016/j.indcrop.2016.02.038
Peighambardoust, S. J., Rowshanzamir, S., & Amjadi, M. (2010). Review of the proton exchange membranes for fuel cell applications. *International Journal of Hydrogen Energy* (Vol. 35). Elsevier Ltd. http://doi.org/10.1016/j.ijhydene.2010.05.017
Pereira, F., Vallé, K., Belleville, P., Morin, A., Lambert, S., & Sanchez, C. (2008). Advanced Mesostructured Hybrid Silica - Nafion Membranes for High-Performance PEM Fuel Cell.

Chemical Materials, *229*(9), 1710–1718.
Rabaey, K., & Verstraete, W. (2005). Microbial fuel cells: Novel biotechnology for energy generation. *Trends in Biotechnology*, *23*(6), 291–298. http://doi.org/10.1016/j.tibtech.2005.04.008
Raghavulu, S. V., Goud, R. K., Sarma, P. N., & Mohan, S. V. (2011). Saccharomyces cerevisiae as anodic biocatalyst for power generation in biofuel cell: Influence of redox condition and substrate load. *Bioresource Technology*, *102*(3), 2751–2757. http://doi.org/10.1016/j.biortech.2010.11.048
Rahimnejad, M., Adhami, A., Darvari, S., Zirepour, A., & Oh, S.-E. (2015). Microbial fuel cell as new technology for bioelectricity generation: A review. *Alexandria Engineering Journal*, *54*(3), 745–756. http://doi.org/10.1016/j.aej.2015.03.031
Schneider, G., Kovács, T., Rákhely, G., & Czeller, M. (2016). Biosensoric potential of microbial fuel cells. *Applied Microbiology and Biotechnology*, *100*(16), 7001–7009. http://doi.org/10.1007/s00253-016-7707-1
Schröder, U., Harnisch, F., & Angenent, L. T. (2015). Microbial electrochemistry and technology: terminology and classification. *Energy and Environmental Science*, *8*(2), 513–519. http://doi.org/10.1039/C4EE03359K
Shah, N., Ul-Islam, M., Khattak, W. A., & Park, J. K. (2013). Overview of bacterial cellulose composites: A multipurpose advanced material. *Carbohydrate Polymers*, *98*(2), 1585–1598. http://doi.org/10.1016/j.carbpol.2013.08.018
Sharaf, O. Z., & Orhan, M. F. (2014). An overview of fuel cell technology: Fundamentals and applications. *Renewable and Sustainable Energy Reviews*, *32*, 810–853. http://doi.org/10.1016/j.rser.2014.01.012
Sotres, A., Tey, L., Bonmat, A., & Viñas, M. (2016). Microbial community dynamics in continuous microbial fuel cells fed with synthetic wastewater and pig slurry. *Bioelectrochemistry*, *111*, 70–82. http://doi.org/10.1016/j.bioelechem.2016.04.007
Stoll, Z. A., Ma, Z., Trivedi, C. B., Spear, J. R., & Xu, P. (2016). Sacrificing power for more cost-effective treatment: A techno-economic approach for engineering microbial fuel cells. *Chemosphere*, *161*, 10–18. http://doi.org/10.1016/j.chemosphere.2016.06.072
Trovatti, E., Serafim, L. S., Freire, C. S. R., Silvestre, A. J. D., & Neto, C. P. (2011). Gluconacetobacter sacchari : An efficient bacterial cellulose cell-factory. *Carbohydrate Polymers*, *86*(3), 1417–1420. http://doi.org/10.1016/j.carbpol.2011.06.046
Ullah, H., Santos, H. A., & Khan, T. (2016). Applications of bacterial cellulose in food, cosmetics and drug delivery. *Cellulose*, *23*(4), 2291–2314. http://doi.org/10.1007/s10570-016-0986-y
Ullah, H., Wahid, F., Santos, H. A., & Khan, T. (2016). Advances in biomedical and pharmaceutical applications of functional bacterial cellulose-based nanocomposites. *Carbohydrate Polymers*, *150*, 330–352. http://doi.org/10.1016/j.carbpol.2016.05.029
Ummartyotin, S., & Manuspiya, H. (2015). A critical review on cellulose : From fundamental to an approach on sensor technology. *Renewable and Sustainable Energy Reviews*, *41*, 402–412. http://doi.org/10.1016/j.rser.2014.08.050
Venkata Mohan, S., Velvizhi, G., Annie Modestra, J., & Srikanth, S. (2014). Microbial fuel cell: Critical factors regulating bio-catalyzed electrochemical process and recent advancements. *Renewable and Sustainable Energy Reviews*, *40*, 779–797. http://doi.org/10.1016/j.rser.2014.07.109
Vilas Boas, J., Oliveira, V. B., Marcon, L. R. C., Pinto, D. P., Simões, M., & Pinto, A. M. F. R. (2015). Effect of operating and design parameters on the performance of a microbial fuel cell with Lactobacillus pentosus. *Biochemical Engineering Journal*, *104*, 34–40. http://doi.org/10.1016/j.bej.2015.05.009
Vilela, C., Gadim, T. D. O., Silvestre, A. J. D., Freire, C. S. R., & Figueiredo, F. M. L. (2016). Nanocellulose/poly(methacryloyloxyethyl phosphate) composites as proton separator materials. *Cellulose*, *23*(6), 3677–3689. http://doi.org/10.1007/s10570-016-1050-7
Waidhas, M., Drenckhahn, W., Preidel, W., & Landes, H. (1996). Direct-fuelled fuel cells. *Journal of Power Sources*, *61*(1–2), 91–97. http://doi.org/http://dx.doi.org/10.1016/S0378-

7753(96)02343-9
Wang, C. (2004). Fundamental Models for Fuel Cell Engineering Fundamental Models for Fuel Cell Engineering. *Chemical Reviews*, *104*(10), 4727–4766. http://doi.org/10.1021/cr020718s
Wang, Y., Chen, K. S., Mishler, J., Cho, S. C., & Adroher, X. C. (2011). A review of polymer electrolyte membrane fuel cells: Technology, applications, and needs on fundamental research. *Applied Energy*, *88*(4), 981–1007. http://doi.org/10.1016/j.apenergy.2010.09.030
Yamada, Y. (2014). Transfer of Gluconacetobacter kakiaceti, Gluconacetobacter medellinensis and Gluconacetobacter maltaceti to the genus komagataeibacter as komagataeibacter kakiaceti comb. nov., komagataeibacter medellinensis comb. nov. and komagataeibacter maltaceti comb. *International Journal of Systematic and Evolutionary Microbiology*, *64*(PART 5), 1670–1672. http://doi.org/10.1099/ijs.0.054494-0
Zhang, H., Chen, B., Xu, H., & Ni, M. (2016). Thermodynamic assessment of an integrated molten carbonate fuel cell and absorption refrigerator hybrid system for combined power Évaluation thermodynamique d ' une pile à combustible intégrée au carbonate fondu et d ' un système hybride de réfrigérateur . *International Journal of Refrigeration*, *70*, 1–12. http://doi.org/10.1016/j.ijrefrig.2016.07.011

6. Appendix

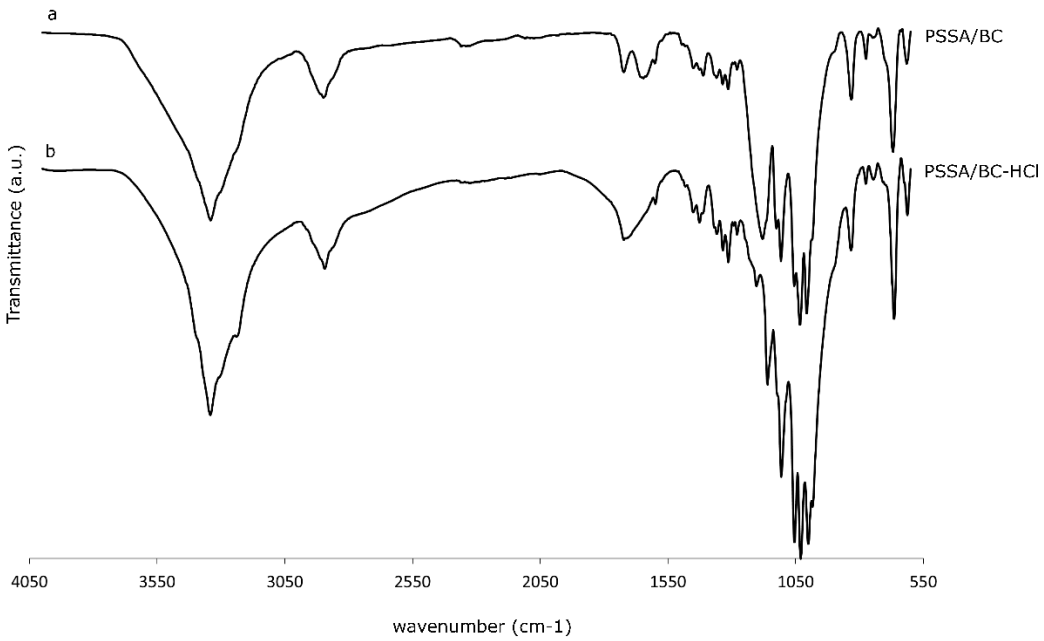

Figure A – FTIR spectra of a PSSA/BC membrane prior, a, and after, b, acidic treatment.

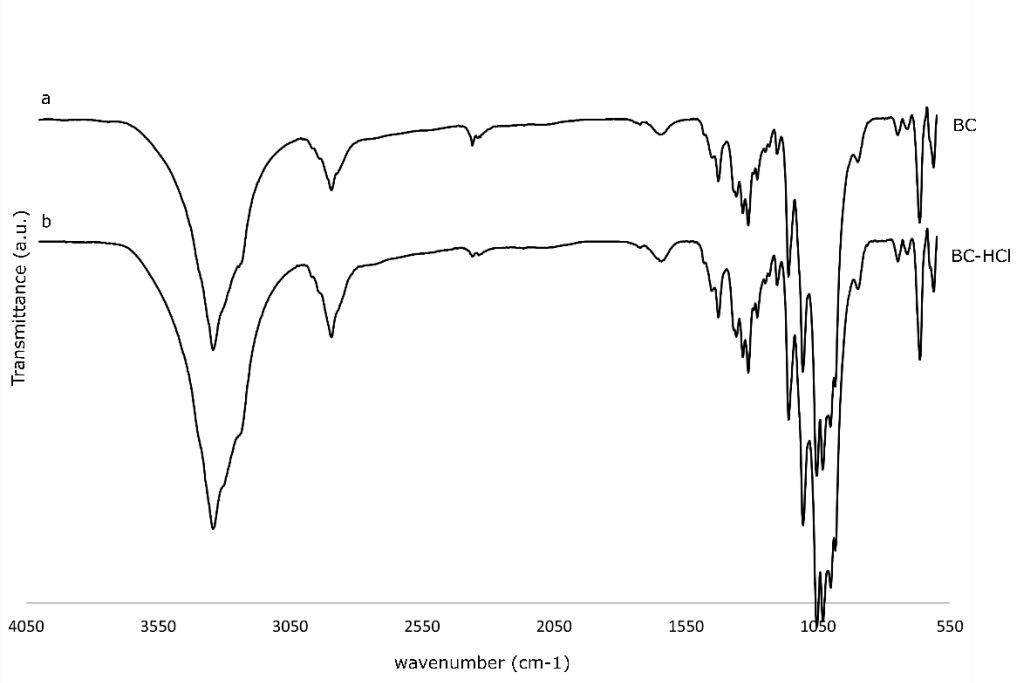

Figure B – FTIR spectra of a BC membrane prior, a, and after, b, acidic treatment.

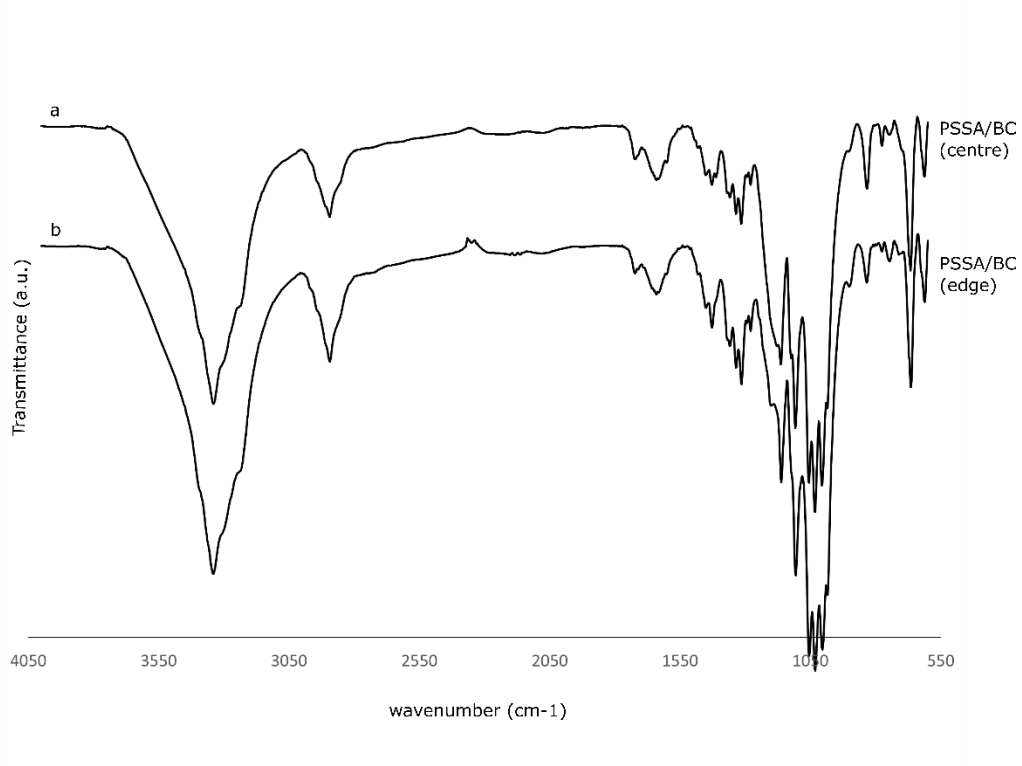

Figure C – FTIR spectra of the centre, a, and edge, b, of a PSSA/BC membrane prior to acidic treatment.

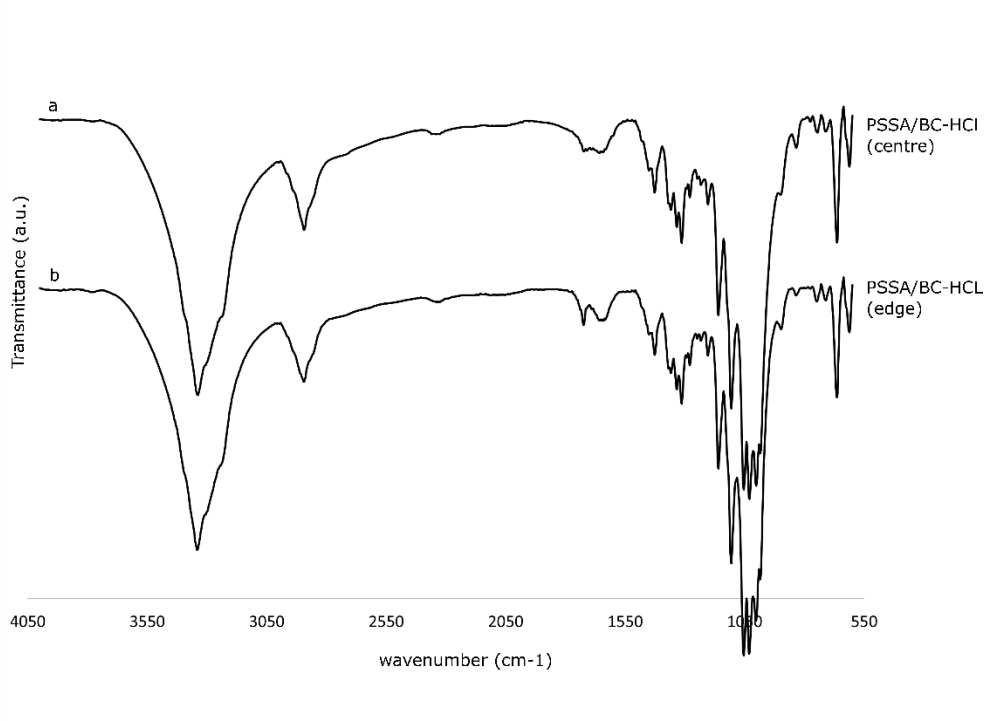

Figure D – FTIR spectra of the centre, a, and edge, b, of a PSSA/BC membrane after acidic treatment.